



NEAR EAST UNIVRSITY

Faculty of Engineering

**Department of Electrical and Electronics
Engineering**

QAM BASED MULTI MEDIA SYSTEM

**Graduation Project
EE- 400**

Student: Hammad Hasan Syed (20002262)

Supervisor: Prof. Dr Fakhreddin Mamedov

NICOSIA 2002

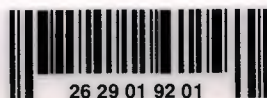




TABLE OF CONTENTS

ACKNOWLEDGMENT	i
LIST OF ABBREVIATIONS	ii
ABSTRACT	iii
INTRODUCTION	iv
1 OVERVIEW OF QAM	1
1.1 Modulation	1
1.2 Amplitude Modulation	2
1.3 Frequency Modulation	2
1.4 Phase Modulation	3
1.5 Coherent and Incoherent Systems	5
1.6 Frequency Shift Keyed	6
1.7 Minimum Shift Keyed	7
1.7.1 Gaussian Minimum Shift Keyed	7
1.8 Phase Shift Keyed	8
1.8.1 Binary Phase Shift Keyed	9
1.8.2 Quadrature Phase Shift Keyed	10
1.8.3 $\pi / 4$ Quadrature Phase Shift Keyed	12
1.8.4 Offset Quadrature Phase Shift Keyed	13
2 SIGNAL PROCESSING	15
2.1 Amplitude Modulation	15
2.1.1 Normal Amplitude Modulation	15
2.1.2 Spectrum of DSB Signals	16



2.2	Detection of QAM Signal	17
2.3	Orthogonal signal sets	19
2.3.1	Simplex Signal Sets	19
2.3.2	Biorthogonal Signal Sets	21
2.3.3	Error Probability Orthogonal Signal Sets	21
2.4	QAM Receiver and Transmitter	23
2.5	Frequency Division Multiplexing	26
2.6	Existing Noise Cancellation Techniques	27
2.7	Active Noise Cancellation	28
2.8	Homogenous Synchronous Dataflow	30
2.9	Performance	31
2.10	Motivation	31
2.10.1	Periodic Non-Gaussian Noise	32

3	QAM CONSTELLATIONS	35
3.1	Introduction	35
3.2	Trellis Coded OFDM System Model	35
3.2.1	Signal Constellation and Mapping for 16-QAM	36
3.2.2	Signal Constellation and Mapping for 32-QAM	37
3.3	System and Channel Descriptions	37
3.4	Analytical and Simulation Results	38
3.4.1	Constant Phase Error	38
3.4.2	Constant Doppler Error	43
3.4.3	Constant Pulse Timing Error	47
3.5	Simulation Results	51
3.5.1	Bit Error Rate Performance	51
3.5.2	BER Performance: Convolution Coded OFDM	54
3.6	Peak to Average Power Ratio	55
3.7	TCM-OFDM	56

4	DIGITAL VIDEO BROADCASTING	57
----------	-----------------------------------	-----------

4.1	Coded orthogonal frequency division multiplexing	57
4.2	Data Rates Using QAM and QPSK	58
4.3	DVB Standards	58
4.3.1	DVB-S	59
4.3.2	DVB-C	59
4.3.3	DVB-T	60
4.3.4	DVB-MS	61
4.4	Processing Of DVB-S	61
4.5	ITU Modem Standards	62
4.5.1	ITU Modems V.22bis	62
4.5.2	V.32bis Standard	63
4.5.3	V.34 and V.34bis Standards	64
4.6	Performance of RS	65
CONCLUSION		68
REFERENCES		69

ACKNOWLEDGEMENTS

I would like to express sincere gratitude to my project adviser professor Dr Fakhheredin Mamedov for his patient and consistent support. Without his encouragement and direction, this work would not have been possible.

I appreciate the help and support extended to me by Mohammad Khurram, Malik Sajid and Imran Haider who were always there for me when ever needed.

All my thanks go to N.E.U staff especially to the Vice President Professor Dr. Shenol Bektash who has always enhanced me in my time of need.

Finally, thanks to Noor, Haroon, Saad, Ali and Ilhan Abi who provided me help and suggestions during the engineering tenure.

LIST OF ABBREVIATIONS

QAM	Quadrature Amplitude Modulation
ASK	Amplitude Shift Keying
PSK	Phase Shift Keying
ATDMA	Advance Time Division Multiple Access
AWGN	Additive White Gaussian Noise
BER	Bit Error Rate
BPSK	Binary Phase Shift Keying
CDMA	Code Division Multiple Access
GMSK	Gaussian Minimum Shift Keying
LP filtering	Low- Phase filtering
MCER	Motion Compensated Error Residual
MPEG	Motion Picture Expert Group
OFDM	Orthogonal Frequency Division Multiplexing
PCM	Pulse Code Modulation
COFDM	Coded Orthogonal Frequency Division Multiplexing
SNR	Signal to Noise Ratio
TCM	Trellis Coded Modulation
TDMA	Time Division Multiple Access
TTIB	Transparent Tone in Band
UTMS	Universal Mobile Telecommunication System
QPSK	Quadrature Phase Shift Keying
AM	Amplitude Modulation
PM	Phase Modulation
SBC	Sub Band Coding

ABSTRACT

The combinations of amplitude shift keying (ASK) and phase shift keying (PSK) is called QAM (quadrature amplitude modulation). Possible variation of QAM is numerous such as 16-QAM, 32-QAM and 64-QAM. The minimum bandwidth required for QAM transmission is the same as that required for ASK and PSK.

Quadrature Amplitude Modulation was developed to overcome the individual constraints of excessively complex AM or PM, by using a combination of the two simultaneously. By combining Phase and Amplitude Modulation at the same time, it is possible to communicate significantly more bits per baud (or symbol) transmitted over the air.

QAM is also being used in the latest upcoming technology named as Coded Orthogonal Frequency Division Multiplexing (COFDM)

This is a more sophisticated and very useful modulation scheme. It is used for all high-speed voice band telephone line modems (e.g. the 14.4 Kbps V.32bis and 33.6 Kbps V.34 standard modems). The idea is to combine amplitude and phase modulation producing multi-level signaling "Constellations". This allows obtaining large M values in practice and therefore increasing the bit rate for a fixed baud rate. As M increases, the advantage of QAM over PSK grows. The constellation in a QAM scheme is the set of amplitude/phase combinations, depicted as points on the complex plane of real and imaginary axes.

INTRODUCTION

In this Project, QAM and some of its based multi-media System such as modems, receivers, transmitters, DVB-T, DVB-C, DVB-S, are studied with intensive care. The Project consists of four chapters.

Chapter 1 gives an over-view of Quadrature Amplitude Modulation which includes Amplitude Modulation, Phase Modulation, and Frequency Modulation in order to get a complete knowledge of basic technique of Modulation.

Chapter 2 gives the basic ideology of Signal Processing relating Quadrature Amplitude Modulation. Important aspects in the Communication and Noise Cancellation are introduced, The transmitting and reception of signals are elaborated by Active and Steady States.

Chapter 3 will cover the possible variations of QAM constellation such as 16-qam, 32-QAM, and 64-QAM and the eradication of Gaussian noise technique has been introduced in the AWGN frame of reference.

Chapter 4 includes a detailed version of digital video broadcasting such as DVB-S, DVB-T, DVB-C, DVB-MS. QAM is also used in the latest and emerging technology i-e Coded Orthogonal Frequency Division Multiplexing (COFDM) which is also discussed in the same chapter.

CHAPTER 1. OVERVIEW OF QAM

1.1 Modulation

Modulation is the process of impressing a low-frequency information signal onto a higher frequency carrier signal. Modulation is done to bring information signals up to the Radio Frequency (or higher) signal. Some systems even have two stage Modulation, where the information is brought up to an Intermediate Frequency (IF), and then increased to the transmission frequency, and then increased to the transmission frequency. Base band Signal is a term used to describe the unmodulated signal or in other words, the information signal. Carrier Signal is what the information signal is combined with to form the new modulated signal. The frequency of the carrier is described as the center frequency of the signal. Both the base band and carrier have bandwidth that matters for AM, but not for FM/PM modulated band width.

Automatic modulation recognition is a rapidly evolving area of signal exploitation with applications in DF confirmation, monitoring, spectrum management, interference identification, and electronic surveillance. Generally stated, a signal recognizer is used to identify the modulation type (along with various parameters such as baud rate) of a detected signal for the purpose of signal exploitation. For example, a signal recognizer could be used to extract.

Signal information useful for choosing a suitable counter measure, such as jamming. In recent years interest in modulation recognition algorithms has increased with the emergence of new communication technologies.

In particular, there is growing interest in algorithms that treat quadrature amplitude modulated (QAM) signals, which are used in the HF, VHF, and UHF bands for a wide variety of applications including FAX, modem, and digital.

1.2 Amplitude Modulation (AM)

Information signal is added and subtracted to and from a carrier signal. Amplitude modulation means a carrier wave is modulated in proportion to the strength of a signal. The carrier rises and falls instantaneously with each high and low of the conversation. Check out the diagram below. See how the voice current produces an immediate and equivalent change in the carrier.

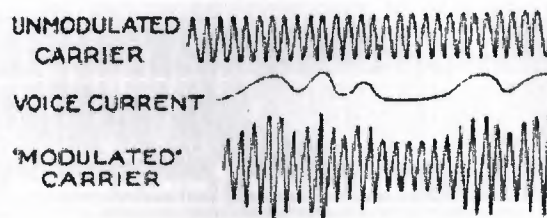


Figure 1.1 Loading the voice on a carrier

Low frequency commercial broadcast stations in the "A.M band" use amplitude modulation. Most C.B. or citizens band radios use it too. It's a simple, robust method to form a radio wave but it suffers from static and high battery power requirements, reasons enough that few personal communications devices use it.

1.3 Frequency Modulation (FM)

Information signal varies a constant Amplitude carrier signal's frequency directly in proportion to the information's frequency.

Frequency modulation confuses many people but it shouldn't. FM is not limited to the FM band. It is not frequency dependent, that is, it can be used at high or low frequencies. That's because it is a modulation technique, a way to shape a radio wave, not a service by itself. The word frequency in FM relates, instead, to the *rate* at which this method varies a carrier wave, not to any particular radio frequency it is used on. This will become clearer as it goes on. The virtues of an FM signal are readily apparent by listening

to the FM band low distortion, little static, good voice quality and immunity from electrical and atmospheric interference. It's why television audio and analog cellular use it. FM also exhibits a capture effect, whereby the receiver seizes on the strongest signal and rejects any others. No other signals fading in and out like with A.M. What's more, F.M. needs far less power to transmit a signal the same distance than A.M.

It doesn't have the modulated carrier varying in amplitude, as with A.M., but in the number of cycles or rate. Although perhaps not obvious at first, the right hand side does differ from the left hand side.

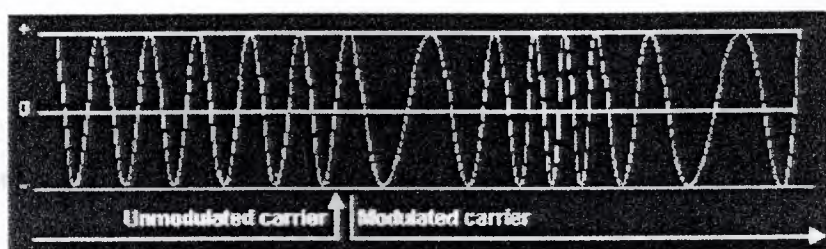


Fig 1.2 The difference in the waveform

Frequency modulation varies the carrier at a rate of 440 cycles per second, matching the original signal. This differs dramatically from A.M. as it is seen above, where a wildly swinging sine wave would be produced instead. In F.M. a quick change in audio frequency results in a quick rate change to the carrier. Despite this seemingly complicated operating method, F.M. circuitry after sixty years is now well established, cheap and simple.

1.4 Phase Modulation (PM)

Information signal varies a constant amplitude carrier signal's phase directly in proportion to the information's frequency. Both FM and PM are form

Three ways exists to modulate a signal: by amplitude, frequency or phase. And although there are dozens of modulation techniques, under the most confusing names possible, all of them will fit into one of these categories. As looked at amplitude modulation, which changes the carrier wave by signal strength, and frequency modulation, which converts the originating signal into cycles? Now if looked at phase modulation,

which changes the angle of the carrier wave. Phase modulation is strictly for digital working and is closely related to F.M. Phase in fact enjoys the same capture effect as F.M.

A digital signal means an ongoing stream of bits, 0s and 1s, on and off pulses of electrical energy. Like those signals running around the inside computer. Well, how do it is transmitted that staccato beat of electrical pulses? one put it on a carrier wave.



Figure 1.3 Scale diagram of a digital signal

One might think that it could send digital without a carrier wave, like the earliest wireless telegraphs but results wouldn't be good.

Radio technology is built on carrier waves. No matter how one transmits RF energy, there is always some type of 'carrier' involved. Ever hear an A.M. radio station go silent for a minute or two? If they are off the air completely would be heard as static. But if they have simply lost audio for a while one will hear a silence. That's the carrier wave.

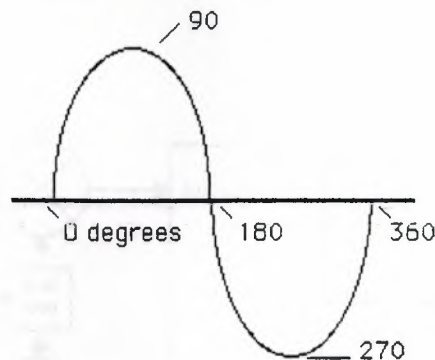


Figure 1.4 Transmission of analog or digital signal

A continuous wave produced to transmit analog or digital information. The phases or angles of a sine wave give rise to different ways of sending information.

1.5 Coherent and incoherent systems

The terms coherent and incoherent are frequently used when discussing the generation and reception of digital modulation. When linked to the process of modulation the term coherence relates to the ability of the modulator to control the phase of the signal, not just the frequency. For example Frequency Shift Keying (FSK) can be generated both coherently with an IQ modulator and incoherently with simply a Voltage Controlled Oscillator (VCO) and a digital voltage source, as shown below.

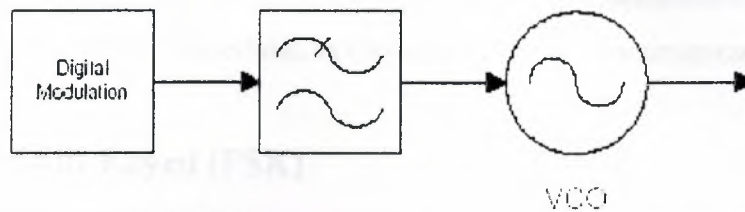


Figure 1.5 In-coherent generation of FSK

With the system in figure 1.5 the instantaneous frequency of the output waveform is determined by the modulator (within a tolerance set by the VCO and data amplitude etc) but the instantaneous phase of the signal is not controlled and can have any value. Alternatively coherent generation of modulation is achieved as shown in figure 1.6. Here the phase of the signal is controlled, rather than the frequency.

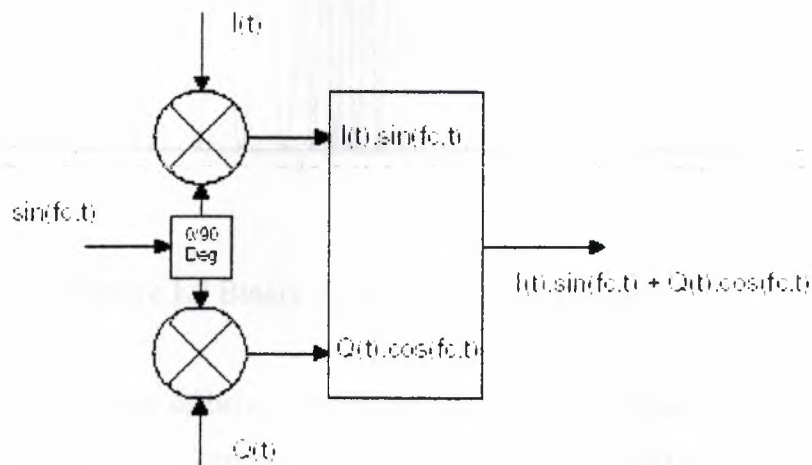


Figure 1.6 Coherent generation of FSK

When a coherent modulator is used to generate FSK the exact signal frequency and phase are controlled. The modulator shown above offers the possibility to shape the resultant carrier phase trajectory at base band either with analogue filtering or digital signal processing and a DAC. This can be used to generate both constant amplitude and amplitude modulated signals. Use of the term coherent with respect to the act of demodulation refers to a system that makes a demodulation decision based on the received signal phase, not frequency. The high level of digital integration now possible in semiconductor devices has made digitally based coherent demodulators common in mobile communications systems.

1.6 Frequency Shift Keyed (FSK)

As previously stated applying modulation in wireless communications involves modifying the phase or amplitude, or both, of a sinusoidal carrier. One of the simplest, and widest used system, is frequency modulation. This exists in a great variety of forms, as will be discussed later, but in essence involves making a change to the frequency of the carrier to represent a different level. The generic name for this family of modulation is Frequency Shift Keying (FSK).

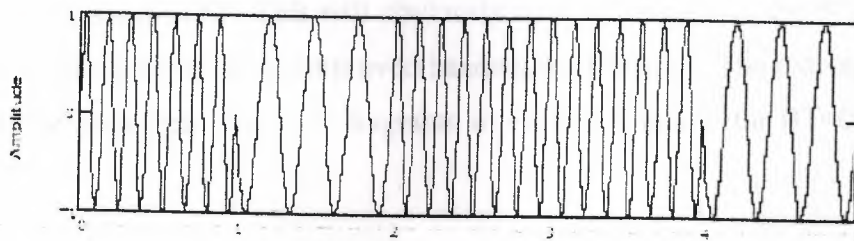


Figure 1.7 Binary (2 level) FSK modulation

FSK has the advantage of being very simple to generate, simple to demodulate and due to the constant amplitude can utilize a non-linear PA. Significant disadvantages, however, are the poor spectral efficiency and BER performance. This precludes its use in this basic form from cellular and even cordless systems.

1.7 Minimum Shift Keyed (MSK)

Minimum Shift Keying is FSK with a modulation index of 0.5. Therefore the carrier phase of an MSK signal will be advanced or retarded 90° over the course of each bit period to represent either a one or a zero. Due to this exact phase relationship MSK can be considered as either phase or frequency modulation. The result of this exact phase relationship is that MSK can't practically be generated with a voltage controlled oscillator and a digital waveform. Instead an IQ modulation technique, as for PSK, is usually implemented. Coherent demodulation is usually employed for MSK due to the superior BER performance. This is practically achievable, and widely used in real systems, due to the exact phase relationship between each bit.

1.7.1 Gaussian Minimum Shift Keyed (GMSK)

A variant of MSK that is employed by some cellular systems (including GSM) is Gaussian Minimum Shift Keying. Again GMSK can be viewed as either frequency or phase modulation. The phase of the carrier is advanced or retarded up to 90° over the course of a bit period depending on the data pattern, although the rate of change of phase is limited with a Gaussian response. The net result of this is that depending on the Bandwidth Time product (BT), effectively the severity of the shaping, the achieved phase change over the bit may fall short of 90° . This will obviously have an impact on the BER, although the advantage of this scheme is the improved bandwidth efficiency. The extent of this shaping can clearly be seen from the 'eye' diagrams in Figure 1.8 below for $BT=0.3$, $BT=0.5$ and $BT=1$.

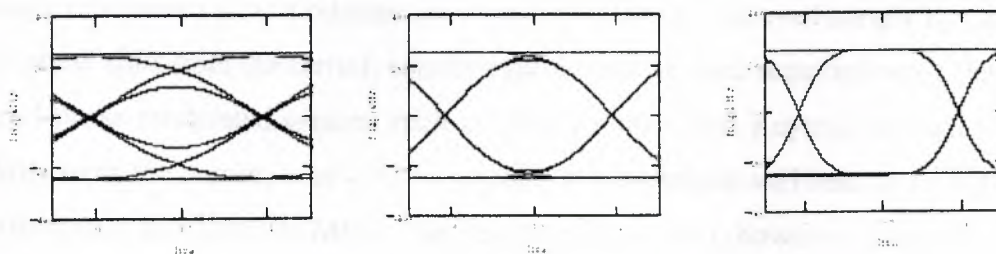


FIGURE 1.8 Eye diagrams for GMSK with $BT=0.3$ (left), $BT=0.5$ (centre) and $BT=1$ (right)

This resultant reduction in the phase change of the carrier for the shaped symbols (i.e. 101 and 010) will ultimately degrade the BER performance as less phase has been accrued or retarded therefore less noise will be required to transform a zero to a one and vice versa. The principle advantages of GMSK, however, are the improved spectral efficiency and constant amplitude. The resulting signal spectra's for $BT = 0.3, 0.5, 1$ and MSK are shown below in Figure

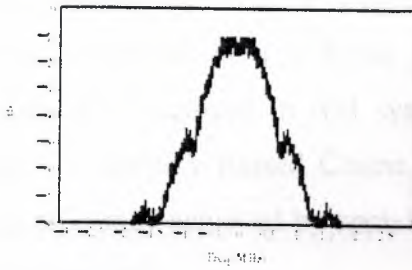


Figure 1.9(a). $BT=0.3$

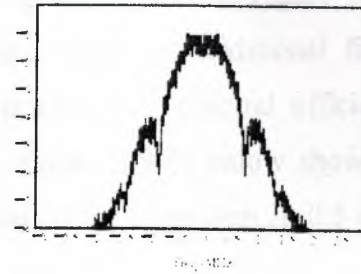


Figure 1.9(b). $BT=0.5$

All the waveforms displayed above (GMSK and MSK) have constant amplitude. That is to say that their quadrature phase trajectory never leaves the unit circle. This can be a significant property, particularly as it allows the Power Amplifier device to be operated further into compression yielding improved efficiency and increased output power, without significant spectral re-growth.

1.8 Phase Shift Keyed (PSK)

An alternative to imposing the modulation onto the carrier by varying the instantaneous frequency is to modulate the phase. This can be achieved simply by defining a relative phase shift from the carrier, usually equi-distant for each required state. Therefore a two level phase modulated system, such as Binary Phase Shift Keying, has two relative phase shifts from the carrier, $+ \text{ or } - 90^\circ$. Typically this technique will lead to an improved BER performance compared to MSK. The resulting signal will, however, probably not be constant amplitude and not be very spectrally efficient due to the rapid phase discontinuities. Some additional filtering will be required to limit the spectral occupancy.

Phase modulation requires coherent generation and as such if an IQ modulation technique is employed this filtering can be performed at base band.

1.8.1 Binary Phase Shift Keyed (BPSK)

The simplest form of phase modulation is binary (two level) phase modulation. With theoretical BPSK the carrier phase has only two states, $\pm \pi/2$. Obviously the transition from a one to a zero, or vice versa, will result in the modulated signal crossing the origin of the constellation diagram resulting in 100% AM. Figure below shows the theoretical spectrum of a 1 Mbits BPSK signal with no additional filtering. Several techniques are employed in real systems to improve the spectral efficiency. One such method is to employ Raised Cosine filtering. Figure 1.9(b) below shows the improved spectral efficiency achieved by applying a raised cosine filter with $\beta=0.5$ to the base band modulating signals.

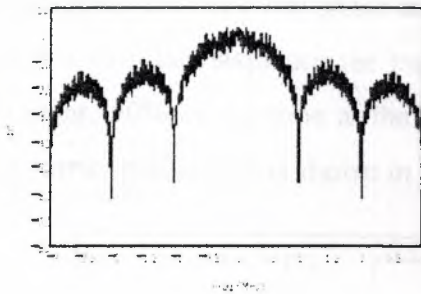


Figure 1.10(a). Theoretical BPSK

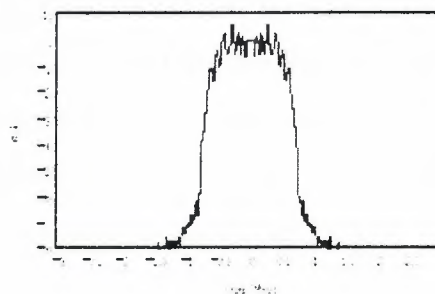


Figure 1.10(b). Raised Cosine BPSK

$$\beta=0.5$$

The improved spectral efficiency will result in some closure of the eye as can be seen in figure 1.11 (a) and 1.11(b).

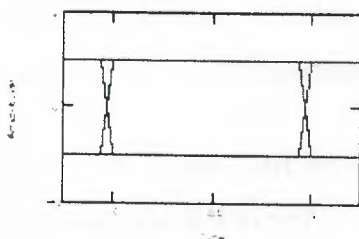


Figure 1.11(a). Theoretical BPSK

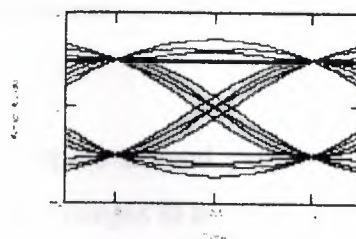


Figure 1.11(b). Raised Cosine BPSK

$$\beta=0.5$$

One potentially undesirable feature of BPSK that the application of a raised cosine filter will not improve is the 100% AM. In a real system the shaped signal will still require a linear PA to avoid spectral re-growth. Further hybrid versions of BPSK are used in real systems that combine constant amplitude modulation with phase modulation. One such example would be Constant Amplitude '50%' BPSK, generated with shaped I and Q vectors designed to rotate the phase around the unit circle between the two constellation points. For a 010 data sequence the trajectory spends 25% of the time traveling from one point to other, 50% of the time at the required point and 25% of the time returning. The resulting carrier phase shift is shown in Figure 1.12 below.

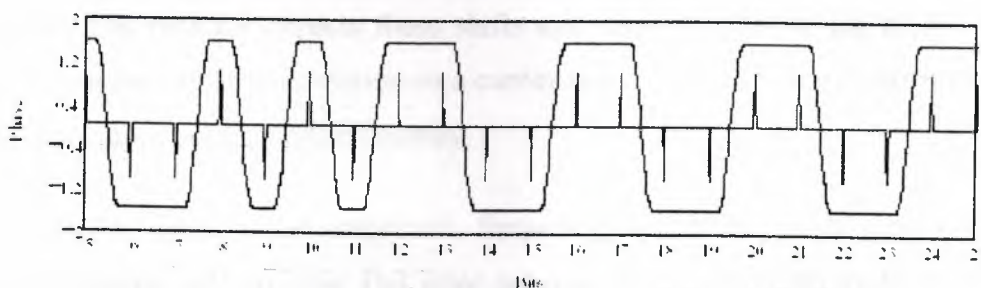


Figure 1.12 Constant amplitude '50%' BPSK.

1.8.2 Quadrature phase shift keying (QPSK)

Let's discuss the awesomely titled quadrature phase shift keying or QPSK. This scheme, used by most high speed modems, allows quicker data transfer than FSK. And it gives at least four states to send information. There's a good chance we have heard this type as our modem makes a dial up connection. IS-136 uses this technology to enable its digital

control channel, allowing PCS like services for conventional cellular. GSM also uses a variation, called, Gaussian Minimum Shift Keying,

Quadrature phase shift keying changes a sine wave's normal pattern. It shifts or alters a wave's natural fall to rest or 0 degrees. By forcing changes in a

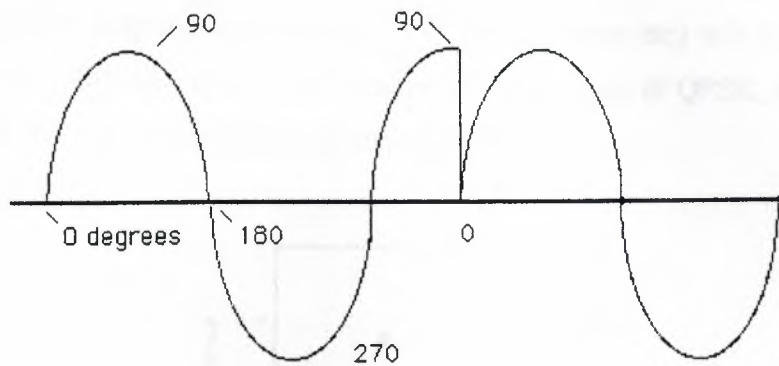


Figure 1.13 As an example, 90 degrees, 0 degrees, 180 degrees, and 270 degrees might be represented by binary digits 00, 01, 10, and 11 respectively.

When arrange the circuit that at each point, it transmits a bit of force a shift in the sine wave. The receiver expects these shifts and decodes them in the proper sequence. Again, by putting digital information on a carrier wave. The shaping of a carrier wave to do this, to carry more pulses more efficiently.

Wireless services use amplitude, frequency, and phase modulation to send both analog and digital radio signals. But what converts an analog signal to digital in the first place? An encoding scheme. Pulse amplitude modulation first measures or samples the strength of an analog signal. Pulse code modulation encodes these plots into binary words, namely 0s and 1s. These binary digits are represented by on and off pulses of electrical energy.

A digital signal thus produced usually modulates the current carrying the signal within a landline. Modulation and pulses, therefore, get digital messages going. Once

completed, the resulting digital signal can be sent over the air with another modulation technique for doing just that.

Higher order modulation schemes, such as QPSK, are often used in preference to BPSK when improved spectral efficiency is required. QPSK utilizes four constellation points, as shown in figure below, each representing two bits of data. Again as with BPSK the use of trajectory shaping (raised cosine, root raised cosine etc) will yield an improved spectral efficiency, although one of the principle disadvantages of QPSK, as with BPSK, is the potential to cross the origin, hence generating 100% AM.

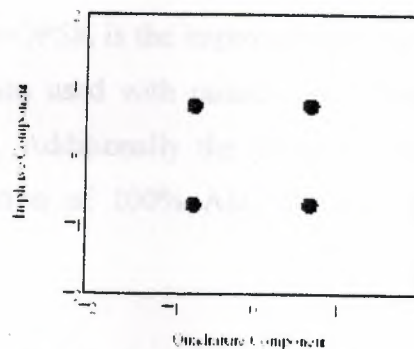


Figure 1.14 Constellation points for QPSK.

1.8.3 $\pi/4$ Quadrature Phase Shift Keyed ($\pi/4$ -QPSK)

A variant of QPSK that is employed in several digital systems is $\pi/4$ -QPSK. As with QPSK two bits are coded onto each symbol, although the quadrature constellations for adjacent bits are offset by $\pi/4$ radians. The two sets of constellation points are shown in figure 1.15.

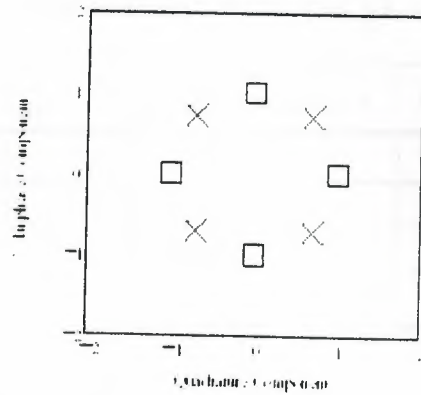


Figure 1.15 Constellation points for $\Pi/4$ -QPSK

One advantage of $\Pi/4$ -QPSK is the improved spectral efficiency, compared to MSK and GMSK, particularly when used with raised cosine phase trajectory shaping due to coding two bits per symbol. Additionally the phase trajectory will no longer cross the origin, avoiding the generation of 100% AM, allowing a harder saturation mode of operation for the PA.

1.8.4 Offset Quadrature Phase Shift Keyed (O-QPSK)

The final variant of QPSK to be considered is Offset Quadrature Shift Keying, or O-QPSK. As previously discussed the potential for a 180° phase shift in QPSK results in the requirement for better linearity in the PA and the potential for spectral re-growth due to the 100% AM. O-QPSK reduces this tendency by adding a time delay of one bit period (half a symbol) in the Quadrature arm of the modulator. The result is that the phase of the carrier is potentially modulated every bit (depending on the data), not every other bit as for QPSK, hence the phase trajectory never approaches the origin. The ability of the modulated signal to demonstrate a phase shift of 180° is therefore removed. As with the other phase modulation schemes considered, shaping of the phase trajectory between constellation points is typically implemented with a raised cosine filter to improve the spectral efficiency. Due to the similarities between QPSK and O-QPSK similar signal spectrum and probability of error are achieved. O-QPSK is utilized in the North American IS-95 CDMA cellular system for the link from the mobile to the base station.

Table 1.1 Distance Properties of PSK Modulations

<i>Modulation</i>	P_{ave}	d_{min}^2 <i>Normalized</i>	<i>SNR Increase</i>
BPSK	1	4.00	–
QPSK	1	2.00	3.00 dB
8-PSK	1	0.5858	5.33 dB
16 PSK	1	0.1522	5.85 dB

were by set

(2.1)

$$(2.2)$$

Where A is a constant, $m(t)$ is the modulating signal, and f_c is the carrier frequency.

The modulation index m is defined as [2.1]

$$m = |\min m(t)|/A \quad (2.3)$$

And the efficiency η of a normal AM signal is defined as [2.2]

$$\eta = P_s/P_t * 100\% \quad (2.4)$$

where P_s is the power carried by the sidebands and P_t is the total power of the normal AM signal.

2.1.1.2 Spectrum of DSB Signals

For double-sideband (DSB) modulation, $A = 0$ and

$$s_c(t) = m(t) \cos 2\pi f_c t \quad (2.5)$$

The Fourier transform of $s_c(t)$ is

$$S_c(f) = 1/2[M(f-f_c) + M(f+f_c)] \quad (2.6)$$

Shows the waveforms and spectra associated with a DSB signal. Clearly, the envelope of the modulated signal does not have the same shape as $m(t)$. As with AM, DSB modulation shifts the spectrum of $m(t)$ to the carrier frequency f_c . The bandwidth of the modulated signal is $2 f_m$ Hz, where f_m is the bandwidth of the modulating signal $m(t)$.

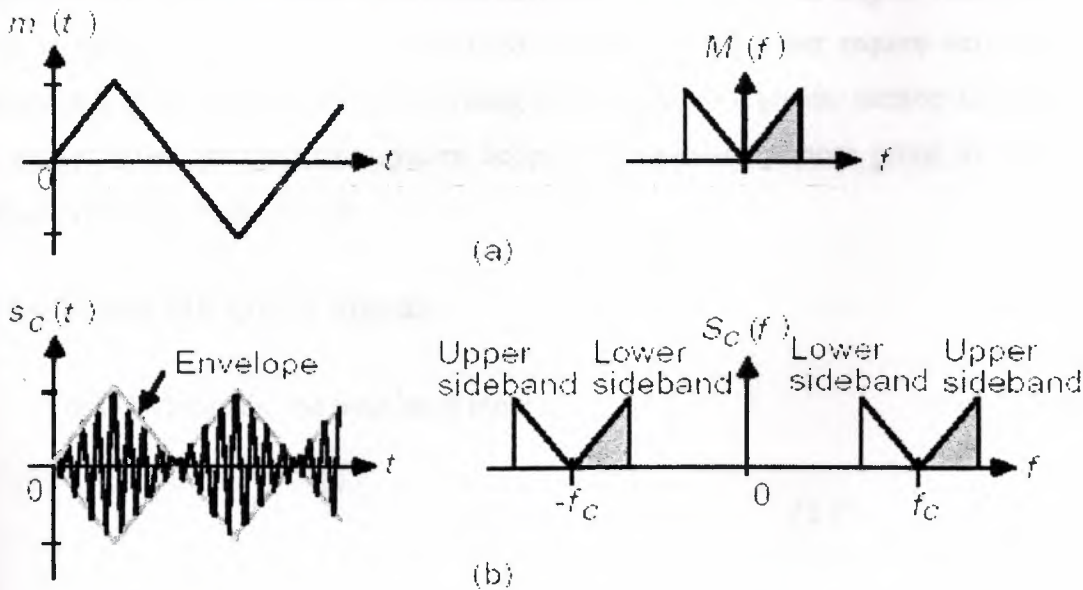


Figure 2.2 Waveforms and spectra associated with DSB signal.

So if the bit stream 001 010 100 011 101 000 011 110 were encoded then the Result would be as shown in figure below:

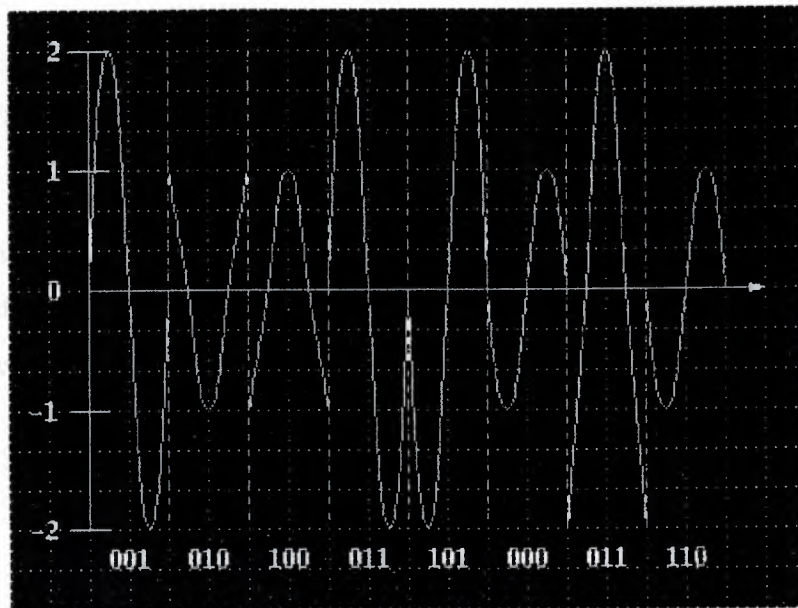


Figure 2.3 QAM Signal

Since both the amplitude and phase shifts can encode larger numbers of bits, it is possible to have large numbers of bits encoded using this method. In Digital Television, 64-QAM is typical. 128-QAM and 256-QAM are also possible but require very accurate equipment to avoid bit errors when decoding takes place; As a greater number of amplitude and phase values are used, the system becomes progressively more prone to noise and attenuation during transmission.

2.2 Detection OF QAM Signal

For QAM signals, the base band input is

$$f(t) = \sum_{j=1}^N A_j p_j(t) \quad (2.7)$$

Where the $\{A_j\}$ are complex and the $\{\theta_j(t)\}$ are orthonormal L_2 vectors over C . We saw that, after modulation to pass band, the real and imaginary parts of the $\{\theta_j(t)\}$ become an orthogonal set at pass band. After demodulation, the received waveform is

$$V(t) = \sum_j V_j \theta_j(t) = \sum_{j=1}^L A_j + Z_j \theta_j(t) + \sum_{j=L+1}^{\infty} Z_j \theta_j(t). \quad (2.8)$$

Under the WGN assumption, the real and imaginary parts of Z_1, \dots, Z_{j_0} are iid and are independent of $Z_{j_0+1}, Z_{j_0+2}, \dots$. By the same argument as above, $v = (v_1, \dots, v_{j_0})^T$ is a sufficient statistic for the detection of A_1, \dots, A_{j_0} . If we view v as a $2j_0$ dimensional real vector,

$$w = (\Re(v_1), \Im(v_1), \Re(v_2), \Im(v_2), \dots, \Re(v_{j_0}), \Im(v_{j_0}))^T$$

And view the input and the noise similarly, it is seen that the ML detection rule, given an observation v , or equivalently w , is to choose the closest possible input hypothesis. In other words, the decision is the hypothesis a_1, \dots, a_{j_0} that minimizes

$$\sum_{j=1}^{j_0} \Re(a_j - v_j)^2 + \Im(a_j - v_j)^2 = \sum_{j=1}^{j_0} |a_j - v_j|^2 \quad (2.9)$$

This says that distance in the j_0 dimensional complex vector space is the same as distance in the corresponding $2j_0$ dimensional real space. ML detection can be viewed equivalently as minimum distance detection over a $2j_0$ dimensional real space or a j_0 dimensional complex space.

It has now reduced the waveform detection problem in WGN to a minimum distance problem over finite dimensional vectors (either real or complex). Is it possible that this problem gets more and more complex as the dimensionality increases? The following theorem, which is a more general form of the theorem of irrelevance, says that, in a sense, the answer is no.

Theorem 2.1 (Theorem of irrelevance) Let $U(t) = \sum_{j=1}^L A_{j,j}(t)$ be the QAM base-band input to a WGN channel. Assume A_1, \dots, A_{j_0} are statistically independent and each have a finite set of equi-probable alternatives. Assume $\{\theta_j(t)\}$ is an orthonormal set over C . Let v

be a sample value of $V = (V_1 \dots V_{j_0})^T$ as given in (2.8). Then the MAP detection for the string A_1, \dots, A_{j_0} of inputs based on the output observation v is the same as the set of j_0 separate MAP detections of A_j based on the observation v_j for each $j, 1 \leq j \leq j_0$.

2.3 Orthogonal signal sets

An orthogonal signal set is a set a_1, \dots, a_m of m real orthogonal m -vectors each with the same energy E . Without loss of generality we choose a basis for \mathbb{R}^m in which the j th basis vector is a_j/\sqrt{E} . Modulation onto an orthonormal set $\{\theta_j(t)\}$ of waveforms then maps hypothesis j ($1 \leq j \leq m$) into the signal a_j and then into the waveform $\sqrt{E}\theta_j(t)$. After Addition of WGN, the sufficient statistic for detection is a sample value y of $Y = A + Z$, where A takes on the values a_1, \dots, a_m with equal probability and $Z = (Z_1, \dots, Z_m)^T$ has iid components $N(0, N/2)$. It can be seen that the MAP and ML decision is to decide on that j for which y_j is largest. The major case of interest for orthogonal signals is where m is a power of 2, say $m = 2^b$.

Thus the signal set can be used to transmit b binary digits, and uses $m = 2^b$ degrees of freedom to do so. The spectral efficiency ρ , (the number of bits per pair of degrees of freedom) is then, $\rho = b/2^b - 1$. It is seen that as m gets large, ρ gets small. What we will show, however, is that as m gets large, we can also make E_b/N_0 small and still have arbitrarily small error probability. In fact, it is shown that E_b/N_0 can be made as close to the Shannon limit of $\ln 2 = 0.693$, i.e., -1.59 dB, while still achieving arbitrarily small error Probability. Before doing that, however, one should discuss two closely related types of signal sets.

2.3.1 Simplex signal sets

Consider the random vector A with orthogonal equi-probable sample values a_1, \dots, a_m as described above. The mean value of A is then

$$\bar{A} = \left(\frac{\sqrt{E}}{m}, \frac{\sqrt{E}}{m}, \dots, \frac{\sqrt{E}}{m} \right)^T.$$

It had been seen that if a signal set is shifted by a constant vector, the Voronoi detection regions are also shifted and the error probability remains the same. However, such a shift can change the expected energy of the random signal vector. In particular, if the signals are shifted to remove the mean, then the signal energy is reduced. A simplex signal set is an orthogonal signal set with the mean removed. That is,

$$S = A - \bar{A}; \quad s_j = a_j - \bar{A}; \quad 1 \leq j \leq m$$

In other words, the j th component of s_j is $\sqrt{E(1-1/m)}$ and each other component is $-\sqrt{E}/m$. Each simplex signal has energy $E(1-1/m)$, so the simplex set has the same error probability as the related orthogonal set, but requires less energy by a factor of $E(1-1/m)$. The simplex set of size m has dimensionality $m - 1$, as can be seen from the fact that the sum of all the signals is 0, so they are linearly dependent. Figure shown below illustrates the orthogonal and simplex sets for

$m = 2$ and 3. For small m , the simplex set is a substantial improvement over the orthogonal set. For example, for $m = 2$, it has a 3 dB energy advantage (it is simply the antipodal one dimensional set) and uses half the dimensions of the orthogonal set. For large m , the improvement becomes almost negligible.

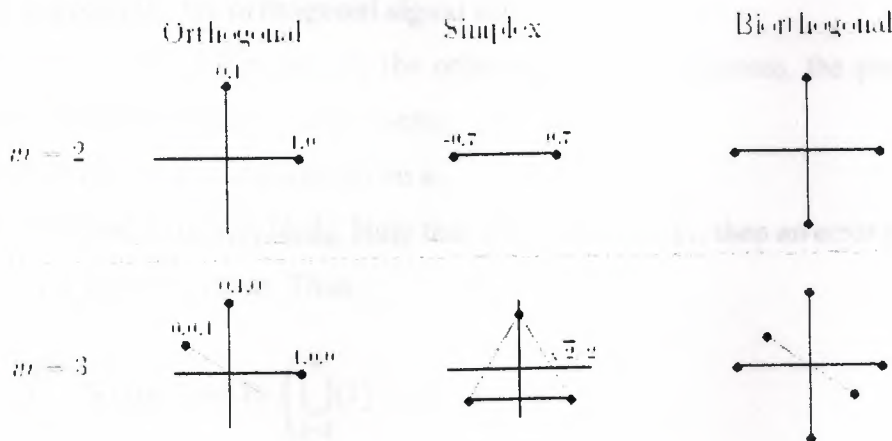


Figure 2.4 Orthogonal, Simplex and Biorthogonal signal constellations

2.3.2 Biorthogonal signal sets

If a_1, \dots, a_m is a set of orthogonal signals, we call the set of $2m$ signals consisting of $a_1, \dots, a_m, -a_1, \dots, -a_m$ a biorthogonal signal set. Two and three dimensional examples of biorthogonal signals sets are given in figure 2.3.

It can be seen by the same argument used for orthogonal signal sets that the ML detection rule for such a set is to first choose the dimension j for which $|y_j|$ is largest, and then choose a_j or $-a_j$ depending on whether y_j is positive or negative. Orthogonal signal sets and simplex signal sets each have the property that each signal is equidistant from every other signal. For biorthogonal sets, each signal is equidistant from all but one of the other signals. The exception, for the signal a , is the signal $-a$. The biorthogonal signal set of m dimensions contains twice as many signals as the orthogonal set (thus sending one extra bit per signal), but has the same minimum distance between signals. It is hard to imagine a situation where it would prefer an orthogonal signal set to a biorthogonal set, since one extra bit per signal is achieved at essentially no cost. However, for the limiting argument it still uses the orthogonal set since it is marginally easier to treat analytically. As m gets very large, the advantage of biorthogonal signals becomes smaller, which is why, asymptotically, the two are equivalent.

2.3.3 Error probability for orthogonal signal sets

Since the signals differ only by the ordering of the coordinates, the probability of error does not depend on which signal is sent;

Thus $\Pr(e) = \Pr(e | A=a_1)$. Conditional on a_1 ,

Y_1 is $N(\sqrt{E}, N_0/2)$ and Y_j is $N(0, N_0/2)$. Note that if $A=a_1$ and $Y_1=y_1$, then an error is made if $Y_j \geq y_1$ for any $j, 2 \leq j \leq m$. Thus

$$\Pr(e) = \int_{-\infty}^{\infty} f_{Y_1|A}(y_1 | a_1) \Pr\left(\bigcup_{j=2}^m (Y_j \geq y_1 | A = a_1)\right) dy_1 \quad (2.10)$$

The rest of the derivation of $\Pr(e)$, and its asymptotic behaviors as m gets large, is simplified if one would normalize the outputs to $W_j = \sqrt{Y_j^2 / N_0}$. Then, conditional on signal 1 being sent, W_1 is $N(\sqrt{2E/N_0}, 1)$ and W_j is $N\{0, 1\}$ for $2 \leq j \leq m$.



$$\Pr(e) = \int_{-\infty}^{\infty} f_{W_1|A}(w_1 | a_1) \Pr\left(\bigcup_{j=2}^m (W_j \geq w_1 | A = a_1)\right) dw_1 \quad (2.11)$$

Using the union bound on the union above,

$$\Pr\left(\bigcup_{j=2}^m (W_j \geq w_1 | A = a_1)\right) \leq (m-1)Q(w_1) \quad (2.12a)$$

It is seen before that the union bound is quite tight when applied to independent quantitative that have small aggregate probability. Thus we expect this bound to be quite tight when w_1 is large. When w_1 is small, however, the bound becomes loose, and even exceeds 1 by a large amount (in the unlikely event that $w_1 = 0$, about half the other hypotheses will be more likely than hypothesis 1). Thus it will upper bound the left side of (4) by 1 when w_1 is small. One can choose the dividing point between large and small w_1 arbitrarily to have a valid upper bound. We would like to choose γ such that $(m-1)Q(\gamma) \approx$

1. Since $\ln[Q(\gamma)] \approx \gamma^2/2$, a convenient choice for γ is $\ln[mQ(\gamma)] \approx 0$

Specifically, γ is defined as

$$\gamma^2/2 = \ln m \quad \gamma = \sqrt{2 \ln m} \quad (2.12b)$$

Using the bound in (4) for $w_1 \geq \gamma$ and using the bound 1 otherwise, (2.11) becomes

$$\Pr(e) = \int_{-\infty}^{\gamma} f_{W_1|A}(w_1 | a_1) dw_1 + \int_{\gamma}^{\infty} f_{W_1|A}(w_1 | a_1) (m-1)Q(w_1) dw_1 \quad (2.13)$$

Since W_1 , given signal 1, is $N(p2E=N_0; 1)$, it is seen that the first term in (2.13) is the lower tail of the distribution of w_1 , and is the probability that the negative of the fluctuation of w_1 exceeds $\sqrt{p2E=N_0} \cdot \gamma$. Thus

$$\int_{-\infty}^{\gamma} f_{W_1|A}(w_1 | a_1) dw_1 = Q(\sqrt{2E/N_0} \cdot \gamma). \quad (2.14)$$

To simplify notation, define $\alpha = \sqrt{2E/N_0}$. Then the first term in (2.13) is simply $Q(\alpha\gamma)$. If one upper bounds $Q(w_1)$ in the second term of (2.13) by

$$Q(w_1) = \frac{1}{2} \exp\left(-\frac{w_1^2}{2}\right) \quad \text{for } w_1 \geq 0 \quad (2.15)$$

This follows from part (a) of exercise 9.4 by using the upper bound $e^{-x^2} \leq 1$ for $x \geq 0$.

Substituting (2.14) and (2.15) into (2.13)

$$\Pr(e) \leq Q(\alpha - \gamma) + \int_{\gamma}^{\infty} \frac{m-1}{2\sqrt{2\pi}} \exp\left(-\frac{(w_1 - \alpha)^2}{2}\right) \exp\left(-\frac{w_1^2}{2}\right) dw_1 \quad (2.16)$$

'Completion of the square' in (2.16) by noting that

$$(w_1 - \alpha)^2 + w_1^2 = 2(w_1 - \alpha/2)^2 + \alpha^2/2 \quad (2.17)$$

Substituting this into (2.16)

$$\Pr(e) \leq Q(\alpha - \gamma) + \left[\frac{m-1}{2\sqrt{2\pi}} \exp\left(-\frac{\alpha^2}{4}\right) \right] \int_{\gamma}^{\infty} \exp(-(w_1 - \alpha/2)^2) dw_1 \quad (2.18)$$

$$\begin{aligned} &= Q(\alpha - \gamma) + \left[\frac{m-1}{2\sqrt{2\pi}} \exp\left(-\frac{\alpha^2}{4}\right) \right] \sqrt{\pi} Q(\sqrt{2}(\gamma - \alpha/2)) \\ &\leq \frac{1}{2} \exp\left[-\frac{(\alpha - \gamma)^2}{2}\right] + \left[\frac{1}{2\sqrt{2}} \exp\left(-\frac{\alpha^2}{4} + \frac{\gamma^2}{2}\right) \right] Q(\sqrt{2}(\gamma - \alpha/2)) \end{aligned} \quad (2.19)$$

where it is being recognized that the final integral in (2.18) is a scaled Q function and then used (2.12b) to upper bound $m-1$ by $\exp(\gamma^2/2)$. It is also assumed that $\alpha > \gamma$ to bound the first term. The analysis now breaks into two special cases, the first where $\gamma > \alpha/2$ and the second where $\gamma \leq \alpha/2$.

2.4 QAM Receiver and Transmitter

Quadrature Amplitude Modulation avoids the spectral inefficiency of double side band amplitude modulation by mapping a stream of bits onto a constellation and modulating the coordinates of the constellation with two orthogonal carriers 90° apart in phase. Thus, the transmitted signal is

$$S(t) = x_p(t) \cos(\omega_c t) - x_q(t) \sin(\omega_c t) \quad (2.20)$$

At the receiver end, $s(t)$ is multiplied by $\cos(\omega_c t)$ and $\sin(\omega_c t)$ to recover the original data, the products are

$$y_p(t) = x_p(t)\cos^2(\omega_c t) + x_q(t)\sin(\omega_c t)\cos(\omega_c t) = \frac{x_p(t)(1 + \cos 2\omega_c t) + x_q(t)\sin 2\omega_c t}{2}$$

$$y_q(t) = -x_p(t)\cos(\omega_c t)\sin(\omega_c t) + x_q(t)\sin^2(\omega_c t) = \frac{-x_p(t)\sin 2\omega_c t + x_q(t)(1 - \cos 2\omega_c t)}{2}$$

The sidebands of the second harmonics of the carriers are then removed by low-pass filtering, and the receiver base band signals $y_p(t)$ and $y_q(t)$ are then within a factor 2 to the originals.

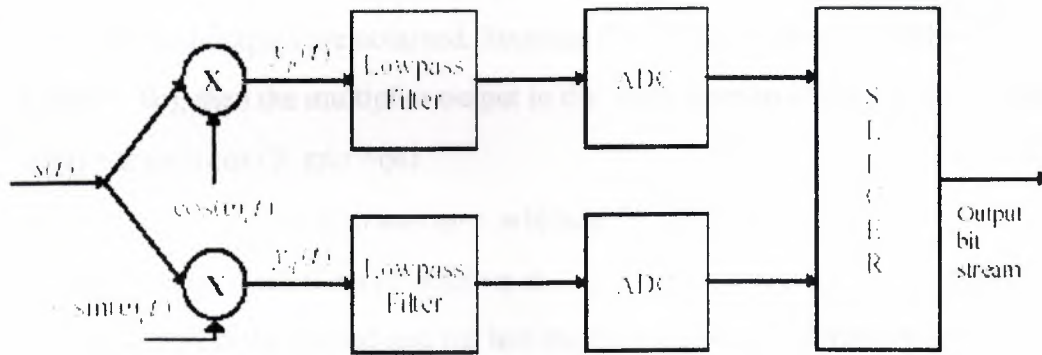


Figure 2.5 QAM Receiver Structure

It is clear that intense computation is needed to multiply $s(t)$ with the carriers and to low pass filter the resulting signals $y_p(t)$ and $y_q(t)$. To reduce unnecessary computation, Schlumberger developed and patented a technique that eliminates the need for signal reconstruction. To increase the transmission band width efficiency, it is possible to send two DSB signals using carriers of same frequency but in phase quadrature. Both modulated signals occupy the same frequency band. Yet they can be separated at the receiver by synchronous detection using two local carriers in phase quadrature. The technique is known as Quadrature Multiplexing and the arrangement is shown in Figure

A QAM signal is given by

$$sc(t) = m1(t) \cos 2 \pi f_c t + m2(t) \sin 2 \pi f_c t$$

At the receiving end, the modulated signal is multiplied by two carriers in phase quadrature.

The signals at the outputs of the multipliers are

$$x_1(t) = 2 s_c(t) \cos 2 \pi f_c t \quad (2.21)$$

$$= m_1(t) + m_1(t) \cos 4 \pi f_c t + m_2(t) \sin 4 \pi f_c t \quad (2.22)$$

and

$$x_2(t) = 2 s_c(t) \sin 2 \pi f_c t \quad (2.23)$$

$$= m_2(t) - m_2(t) \sin 4 \pi f_c t + m_1(t) \sin 4 \pi f_c t \quad (2.24)$$

If we suppress the high-frequency components by low-pass filters, we get

$$y_1(t) = m_1(t)$$

And

$$y_2(t) = m_2(t)$$

That is, the desired outputs are obtained. Suppose that the local carrier signal is $\cos(2 \pi f_c t + \theta_0)$, then the multiplier output in the upper portion of the circuit becomes

$$x_1(t) = 2 s_c(t) \cos(2 \pi f_c t + \theta_0) \quad (2.25)$$

$$= m_1(t) \cos \theta_0 + m_1(t) \cos(4 \pi f_c t + \theta_0) -$$

$$m_2(t) \sin \theta_0 + m_2(t) \sin(4 \pi f_c t + \theta_0) \quad (2.26)$$

If we suppress the second and the last terms by a low-pass filter, we get

$$y_1(t) = m_1(t) \cos \theta_0 + m_2(t) \sin \theta_0 \quad (2.27)$$

The desired signal $m_1(t)$ and the unwanted signal $m_2(t)$ appear in the upper portion of the circuit. Also, it can be shown that $y_2(t)$ contains the desired signal $m_2(t)$ and the unwanted signal $m_1(t)$. Modulated signals having the same carrier frequency now interfere with each other. This is called co channel interference and must be avoided. Similar problems arise when the local carrier frequency is in error. Therefore, the local carrier must not only be of the same frequency but must be synchronized in phase with the carrier signal. A slight error in the frequency or the phase of the local carrier signal will result not only in loss and distortion of signals, but will also lead to interference. Quadrature multiplexing is used in color television to multiplex the signals which carry the information about colors.

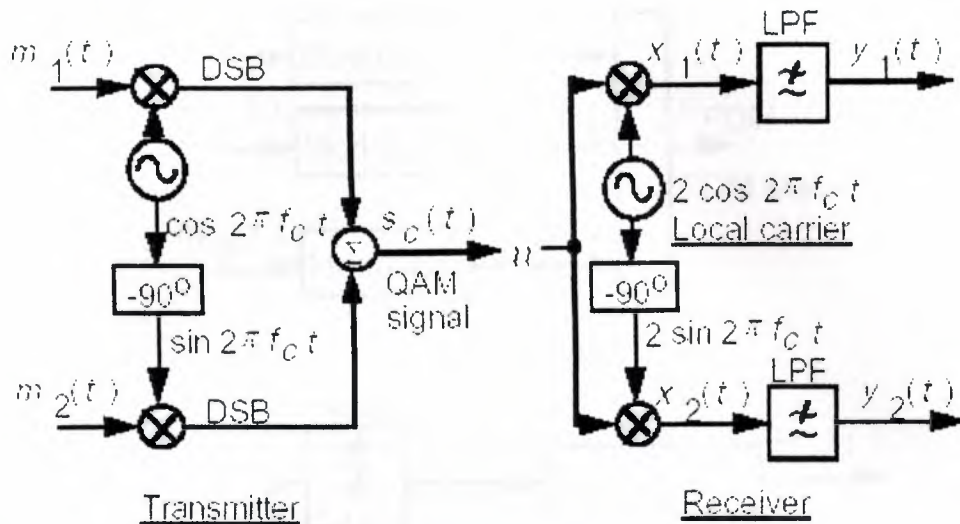
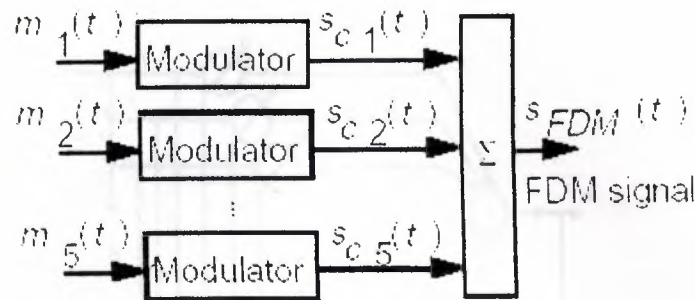


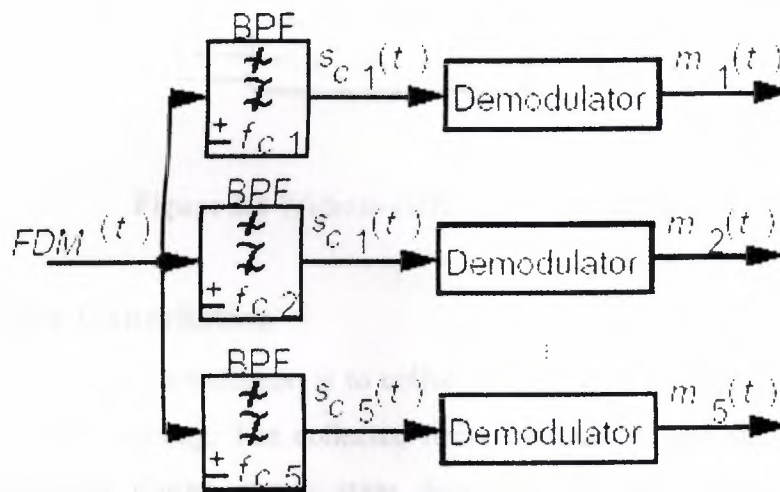
Figure 2.6 A QAM Transmitter and Receiver

2.5 Frequency Division Multiplexing (FDM)

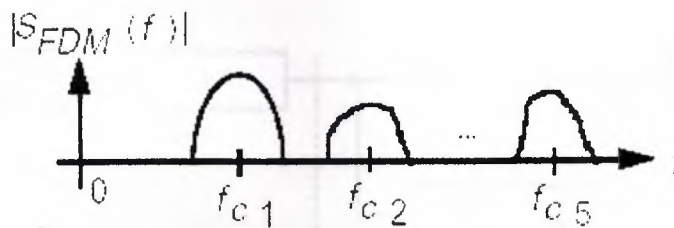
One of the basic problems in communication engineering is the design of a system which allows many individual signals from users to be transmitted simultaneously over a single communication channel. The most common method is to translate individual signals from one frequency region to another frequency region. Suppose that one had several different signals of the same bandwidth. If they translate each one of the signals to a different frequency region such that the translated signal spectra do not overlap each other, then all these signals can now be transmitted along a single communication channel. At the receiving end, the signals can be separated and recovered. Which is known as frequency multiplexed system. Such a multiplexing technique is called frequency division multiplexing (FDM). Frequency translation can be accomplished by multiplying a low frequency modulating signal with a high-frequency sinusoidal carrier signal. Figure 2.6 shows the transmitter, the receiver, and the spectrum of a 5-user FDM system with carrier frequencies $f_{c1} < f_{c2} < \dots < f_{c5}$.



(a) Transmitter



(b) Receiver



(c) Spectrum of FDM signal

Figure 2.7 FDM system

2.6 Existing Noise Cancellation Techniques

Early research has been done in the noise cancellation area. The most famous work is perhaps the Least Mean Square Algorithm, illustrated in Figure 2.7, introduced by Widrow and Hoff [Widrow 75] in the mid 70s. However, the LMS algorithm presented by Widrow was aimed at removing single tone interference and not periodic wideband noise.

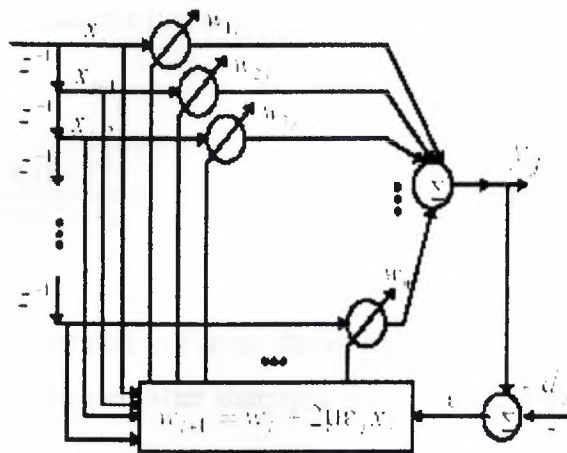


Figure 2.8 Widrow-Hoff LMS Algorithm.

2.7 Active Noise Cancellation

The idea of noise cancellation is to collect an estimation of the periodic wideband noise during receiver training. The collected noise estimate is then subtracted from the received QAM signal during steady state data transmission. Figure 2.9 is a block representation of the receiver operation during training.

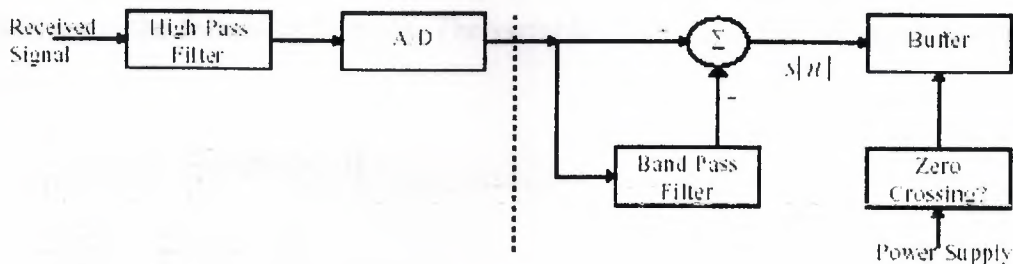


Figure 2.9 Receiver operations during training

The structure to the right of the dash line is responsible for noise extraction. The transmitted signal is known during receiver training, for example, the signal can be a 52.5 kHz tone. It is clear that with the transmitted signal known a priori, noise estimate can be computed as noise Estimates $n = \text{Actual received signal} - \text{Training signal}$. Furthermore, the training signal can be extracted at the receiver using a narrow band notch filter centered at

the carrier frequency 52.5 kHz. The notch filter is implemented using a second-order IIR bi quad with the following transfer function.

$$\frac{Y(z)}{S(z)} = \frac{k_0(1 - z^{-1})}{1 - k_1 z^{-1} - k_2 z^{-2}} \quad (2.28)$$

The filter structure is illustrated in Figure shown below The coefficients k_0 , k_1 , and k_2 can be adjusted to obtain the desired filter sharpness and filter build-up time

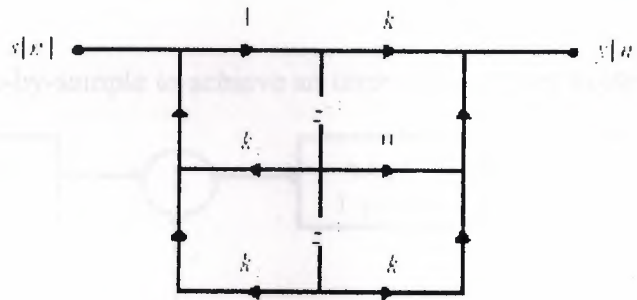


Figure 2.9 IIR bi quad band pass filter

The buffer block in Figure2.9 can be implemented using a circular buffer and updated using the following formula. The variable i represents the i th sample in the 60 Hz noise cycle.

$$\begin{aligned} [n] &= \frac{\alpha}{\beta} s[n] + (1 - \frac{\alpha}{\beta}) \text{buffer}_i[n-1] \\ &= \frac{\alpha}{\beta} \left[\sum_{k=0}^{N-1} (1 - \frac{\alpha}{\beta})^k s[n-k] \right] \end{aligned} \quad (2.29)$$

N is the number of 60 Hz noise cycles during training duration. The ratio α/β is the Buffer update factor and must be chosen carefully to optimize the cancellation algorithm. From Equation 2.29, it is clear that if the update factor is zero, then no update is made to the noise buffer and it retains its initial values. If the factor is one, then only the most current noise cycle is kept. Therefore, an update factor close to zero implies that the noise estimate will be approximately a running average while a factor close to one means that the

most recent noise cycle will be weighted more. Averaging is a more conservative approach but the noise estimate will remain valid for a longer duration. On the other hand, an emphasis on more recent noise cycles is an aggressive approach that will produce a better result in the short term in exchange for the need to frequently reacquire the noise pattern which may not be possible during steady state.

The zero-crossing block in Figure 2.9 is used to combat 60 Hz crosstalk drift. Whenever the positive zero-crossing occurs in the power supply, the zero-crossing block will reset the buffer pointer to the head of the buffer array, i.e. sample number one of the noise estimate. Actual noise cancellation occurs in steady state. Figure 2.30 is a block diagram of the receiver operation during steady state. The noise estimate is subtracted from the received

QAM signal sample-by-sample to achieve an improved receiver noise performance.

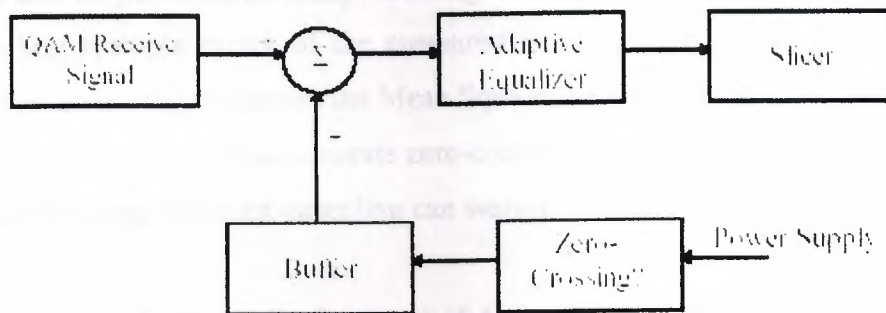


Figure 2.30 Noise cancellations in steady state

2.8 Homogeneous Synchronous Dataflow

Synchronous Dataflow (SDF) is a well-suited model of computation for digital communications systems which often process an endless supply of data. The simplest form of an SDF is a homogeneous SDF graph where the number of tokens consumed and produced on each arc is a constant one. HSDF fits nicely with the specification of Active Noise Cancellation. Figure 2.31 illustrates the algorithm using an HSDF graph. The actor firing sequence will be {ADC Read, Int-to-Float, Notch Filter, Estimate Noise, Zero-Crossing, Buffer Write} during training and {ADC Read, Int-to-Float, Cancel Noise, Zero-Crossing} during steady state.

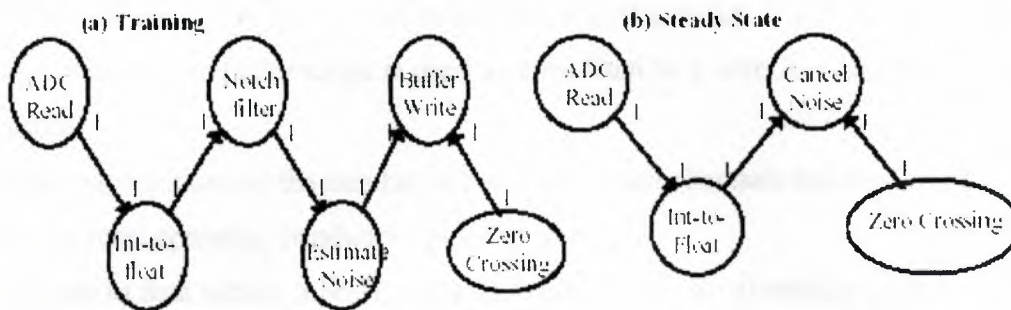


Figure 2.31. HSDF graph representation of receiver operation in (a) training and (b) steady state.

2.9 Performance

Active Noise Cancellation has been simulated using Analog Device's SHARC simulator and its performance analyzed using MATLAB. Crosstalk interference is created by appending multiple cycles of the measured noise, seen in Figure 2.32. Active Noise Cancellation on average improves the Mean Square Error by 7dB as illustrated in Table 2.1. Also notice from the table that accurate zero-crossing information is crucial to proper noise cancellation because incorrect canceling can worsen the noise.

Table 2.1 Performance of Active Noise Cancellation.

Method	Average MSE	Average SNR
Required values under Gaussian noise to obtain an BER of 10	-35 dB	35 dB
No Active Noise Cancellation	-25 dB	25 dB
Active Noise Cancellation <i>without</i> Zero-Crossing information	-23 dB	23 dB
Active Noise Cancellation <i>with</i> Zero-Crossing information	-32 dB	32 dB

2.10 Motivation

One of the many challenges that one can face in wire line telemetry is how to operate high-speed data transmissions over non-ideal, poorly controlled media. The key to any telemetry system design depends on the system's ability to adapt to a changing environment. While adaptive equalization can account for frequency-dependent cable attenuation by inverting channel distortion there still exists the need to reduce other sources

of noise, for example, the near-end crosstalk (NEXT) that exists in a multi-conductor cable. Typically, a multi-conductor cable is used as a medium in a wire line telemetry system for two reasons:

1. Multiple cables increase the number of communication channels and therefore increase the total operating bandwidth of the system.
2. In addition to data cables, a power cable is needed to supply electricity to the telemetry transmitter at the remote end.

The principal source of interference is now the coupling between the power cable and data cable. This noise is far from white and can reduce the SNR by more than 10 dB, an amount that can severely hamper the telemetry system's performance. The structure of the paper is as follows.

First we discuss the observed periodic non-Gaussian noise and explain why it is difficult to reduce this noise using frequency domain filtering. Next, we introduce an innovative time domain approach, Active Noise Cancellation that can reduce in-band crosstalk without distorting the signal of interest.

Finally, we outline the specification of this cancellation algorithm using a homogeneous synchronous dataflow (HSDF) graph and describe its implementation on an embedded DSP processor.

2.10.1 Periodic non-Gaussian noise

The crosstalk interference can be described as a collection of noise pulses superimposed on top of a slow varying 60 Hz sine wave originated from the power supply.

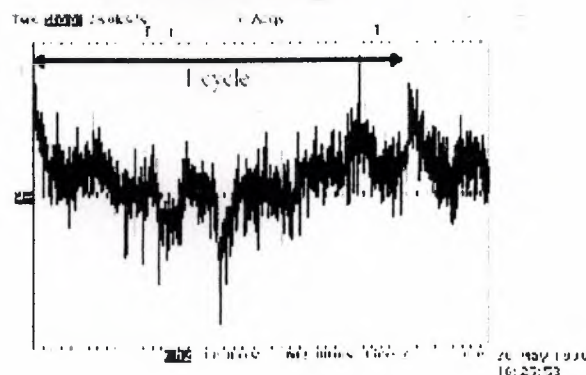


Figure 2.32 Oscilloscope capture of approximately one cycle of crosstalk

Figure 2.32 is an oscilloscope capture of the actual crosstalk interference. The double arrow line above the figure approximately marks one period of the 60 Hz crosstalk. To better describe the effective noise one can decouple the crosstalk into a 60 Hz sine component and a collection of periodic noise pulses as seen in Figure 2.33

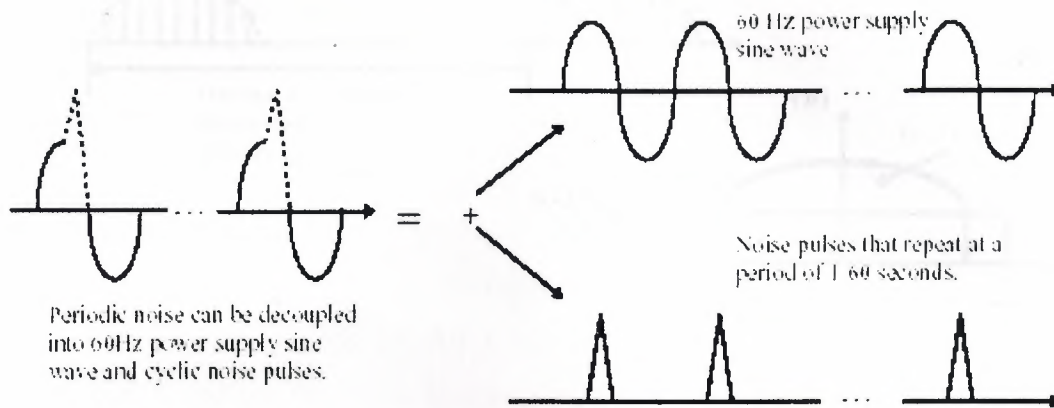


Figure 2.33 Decoupling of crosstalk into 60Hz sine component and periodic noise pulses

Each of the noise pulses in Figure 2.33 is a collection of impulses as shown in Figure 2.34(a). Hence the crosstalk creates a non-Gaussian noise, because the noise is periodic, that maps to a wideband noise in the frequency domain, because the noise consists of impulses in the time domain. The wideband noise completely overlaps the transmitted QAM signal which has a bandwidth of, for example $f_b = 70$ KHz and is modulated by a carrier off $c = 525$ kHz as seen in figure 2.34(b).

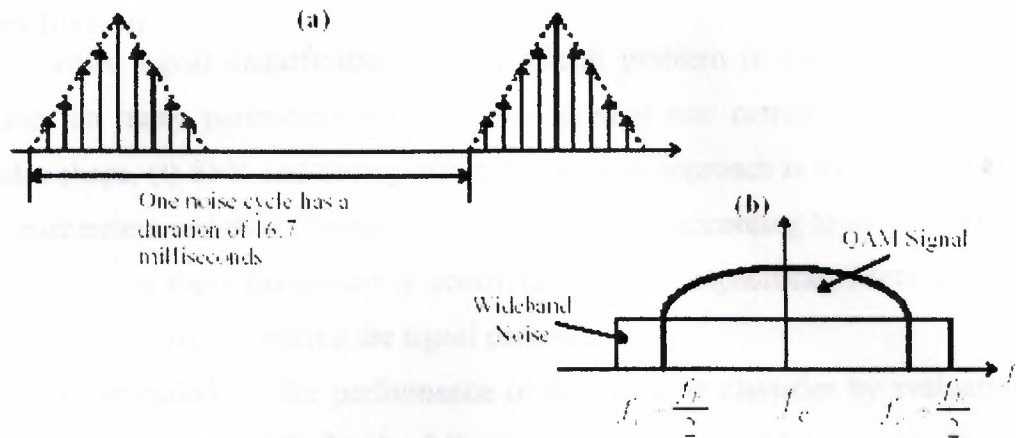


Figure 2.34.(a) Each 60 Hz noise cycle consists of a group of sampled impulses
(b)QAM signal with over lapping wide band noise

As a result, frequency domain filters cannot remove the wideband noise without actually removing the desired QAM signal as well and frequency domain filtering becomes an ineffective approach to eliminating the periodic crosstalk noise.

3. QAM CONSTELLATION

3.1 Introduction

Automatic signal classification rather difficult problem in composite hypothesis testing since so many parameters are unknown: symbol rate carrier frequency, carrier phase, pulse shape, (t) SNR and timing offset. A common approach is to first estimate the unknown parameters and then attempt to classify the signal according to modulation type. Although estimating these parameters is nontrivial, it is not impractical. There are a wide variety of techniques for estimating the signal parameters.

The investigation for the performance of the coherent classifier by evaluating its error rate as a function of SNR for the following PSK/QAM modulation types QAM-16, QAM-32 and QAM-64. For QAM however, there are many possibilities including rectangular and circular configurations. We consider the rectangular configurations defined

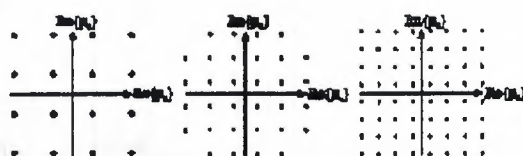


Figure 3.1 16-QAM 32-QAM 64-QAM

3.2 Trellis Coded OFDM System Model

Figure 3.2 shows the trellis coded OFDM system model. TCM encoder is placed at the very first stage and then output serial bit stream is converted to parallel bit stream (block length M , size of M is depend on the modulation scheme used) at the serial to parallel (S/P) converter. Out of M bits, x bits [$M = 512 \cdot x$] are applied to signal mapper and digitally modulated output is available at the signal mapper output. It is interesting to note that, different modulation schemes can be used on different sub channels for layered services. But here it is assumed that the all sub-channels are modulated with the same modulation scheme. Output of the signal mapper will then be applied to partial transmit sequence (PTS) based IFFT processor which will perform four IFFT sets. Each IFFT set is multiplied by a rotation factor $(1, -1, j, -j)$ at the stage of phase rotation such that peak to average power will be minimized for a transmitted block. Finally output of the phase

rotation block will be sent to parallel to serial (P/S) converter to make the output a serial data stream. Figures 3.3 and 3.4 show the encoder structures for 16-QAM and 32-QAM respectively.

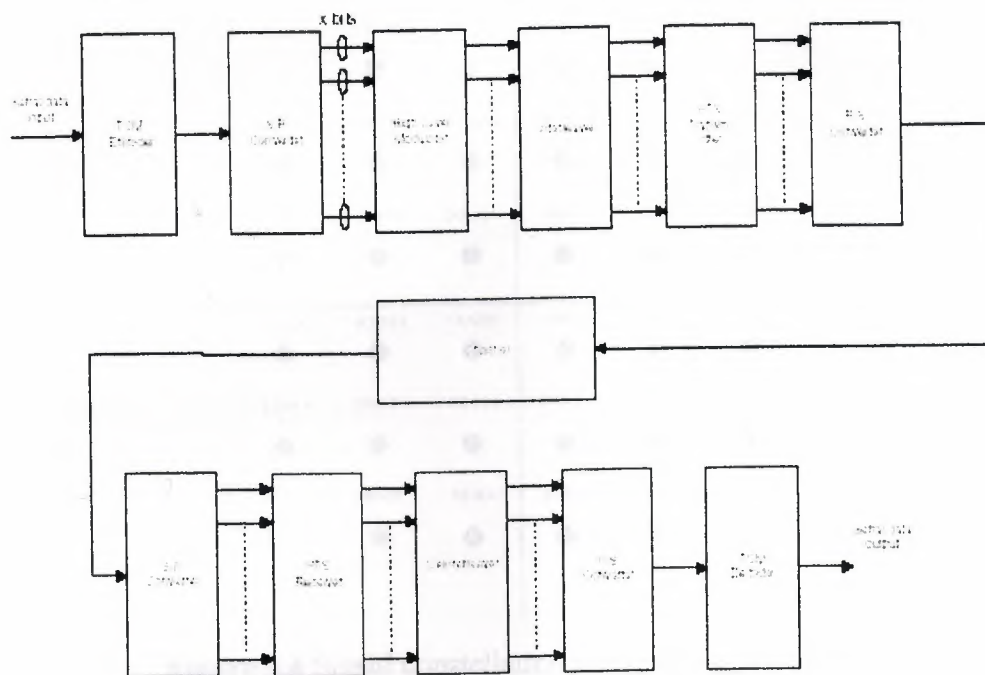


Figure 3.2 Trellis coded OFDM simulated system model

3.2.1 Signal Constellations and Mapping for 16-QAM

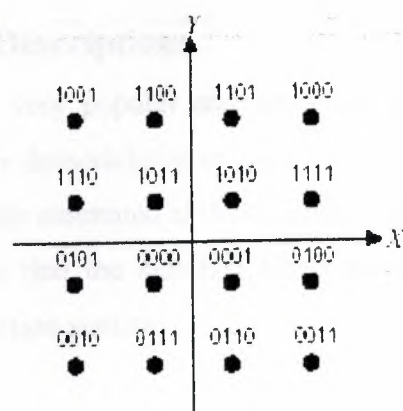


Figure 3.3 Signal constellation and mapping for 16-QAM

3.2.2 Signal Constellations and Mapping for 32-QAM

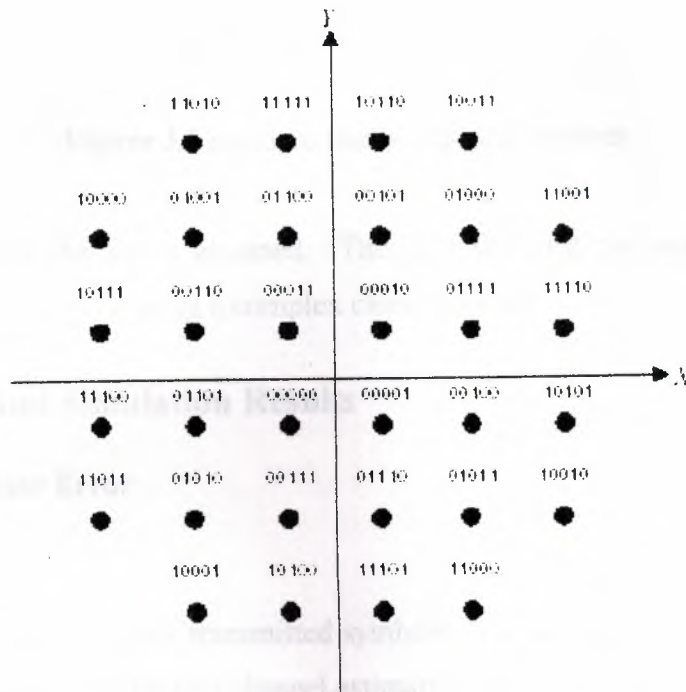


Figure 3.4 Signal constellation and mapping for 32-QAM

Figures 3.3 and 3.4 show the signal mapping and constellation for 16-QAM and for 32 cross QAM [17]. In all TCM-OFDM simulations the above mapping and Constellations are used.

3.3 System and Channel Descriptions

QAM modulation is a very popular and spectrally efficient modulation scheme. However, it must be coherently demodulated in the receiver. Therefore, the carrier phase and frequency must be accurately estimated at the receiver. Additionally, an estimate of the pulse time must be formed so that the matched filters in the receiver can be optimally sampled for the necessary detection statistic.

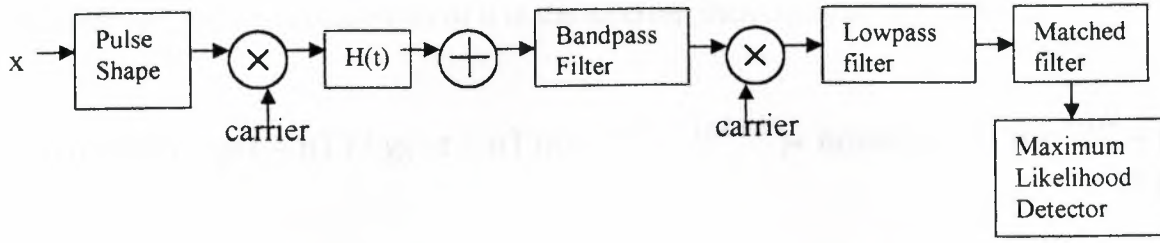


Figure 3.5 standard transmitter and receiver

A flat fading channel is assumed. This is a standard transmitter/receiver setup. Much of the analysis is done using a complex channel model.

3.4 Analytical and Simulation Results

3.4.1 Constant Phase Error

- In AWGN:

Let $d(n)$ be the complex transmitted symbols. By complex base band analysis the received symbols, assuming perfect channel estimation are:

$$r(n) = d(n) + \text{noise}(n) \quad (3.1)$$

In AWGN, the noise is complex Gaussian noise. The real and imaginary parts both have a variance of the square root of $(N_0/2)$.

The transmitted signal can be represented as:

$$\text{Re}\{d(n)g(t - nT)e^{-j\omega t}\} + \text{noise} \quad (3.2)$$

The ideal receiver has a local oscillator that can be represented as $e^{+j\omega t}$. The received complex symbols after demodulation and pulse shaping are therefore:

$$r(n) = d(n)(g(t - nT) * g(-t - nT))(e^{-j\omega t}e^{+j\omega t}) + \text{noise}(n) = d(n) + \text{noise}(n) \quad (3.3)$$

If, however, there is a phase bias of θ in the receiver, then equation 3 becomes:

$$r_{\theta}(n) = d(n)(g(t - nT) * g(-t - nT))(e^{-j\omega t} e^{+j\omega t + \theta}) + \text{noise}(n) = d(n)e^{+j\theta} + \text{noise}(n) \quad (3.4)$$

The received constellation is therefore rotated by θ . The received constellation is now:

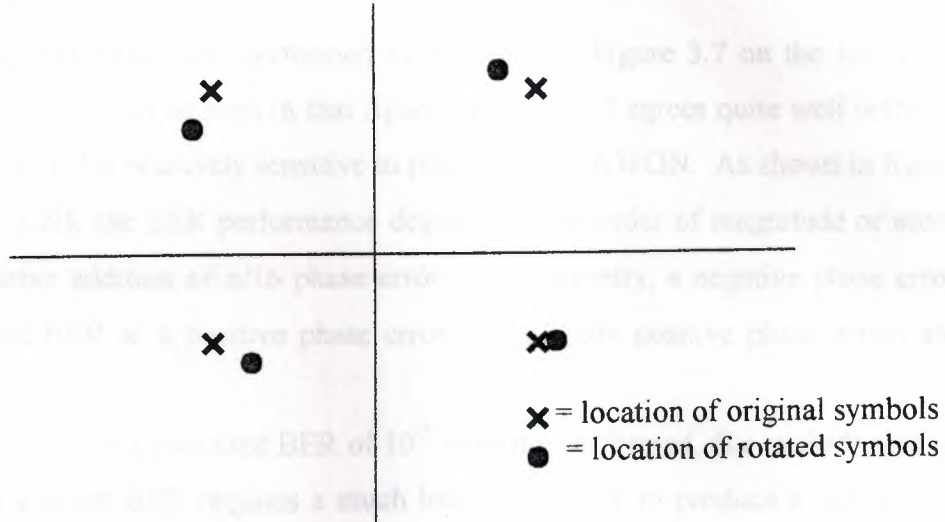


Figure 3.6 Received constellation

By simple geometry, if the original symbol in the first quadrant is located at $(1 + j)$, then the rotated symbol is at

Rotated Symbol =

$$(\sqrt{2})(\cos(\frac{\pi}{4} + \theta) + j\sin(\frac{\pi}{4} + \theta)) = (\sqrt{2})(\sin(\frac{\pi}{4} - \theta) + j\sin(\frac{\pi}{4} + \theta)) \quad (3.5)$$

Similar equations can be derived for each quadrant. The effect of this is that in each quadrant, one bit has its amplitude amplified by $(\sqrt{2})(\sin(\frac{\pi}{4} + \theta))$, and the other bit attenuated by $(\sqrt{2})(\sin(\frac{\pi}{4} - \theta))$. As shown in [3.9],

$$P_{b, \text{unrotated}} = Q(\sqrt{2\gamma_b}) \quad (3.6)$$

However, since half the bits have increased amplitude and the other half have decreased amplitude:

$$\begin{aligned}
 P_{\text{rotated}} &= 0.5Q(\sqrt{2\gamma_b}\sqrt{2}\sin(\frac{\pi}{4} + \theta)) + 0.5Q(\sqrt{2\gamma_b}\sqrt{2}\sin(\frac{\pi}{4} - \theta)) \\
 &= 0.5\{Q(2\sqrt{\gamma_b}\sin(\frac{\pi}{4} + \theta)) + Q(2\sqrt{\gamma_b}\sin(\frac{\pi}{4} - \theta))\} \quad (3.7)
 \end{aligned}$$

A Mat lab simulation was performed to verify this. Figure 3.7 on the following page gives the results. It can be seen in that figure, equation 3.7 agrees quite well with the simulated values. QAM is relatively sensitive to phase error in AWGN. As shown in figure 3.7, at $E_s/N_0 = 13$ dB, the BER performance degrades by an order of magnitude or more with each successive addition of $\pi/16$ phase error. By symmetry, a negative phase error produces the same BER as a positive phase error. Thus, only positive phase errors are shown.

Simulations below a predicted BER of 10^{-5} were not performed, due to the length of time required, as a lower BER requires a much longer sequence to produce a statistically valid result. The plot shown took several hours run time on the TREE servers to produce.

As a final note, this analysis does assume that the phase error is less than $\pi/4$. At a phase error of $\pi/4$ or greater, the constellation has rotated to or beyond the decision boundaries. So, one bit is expected to be in error at least half the time.

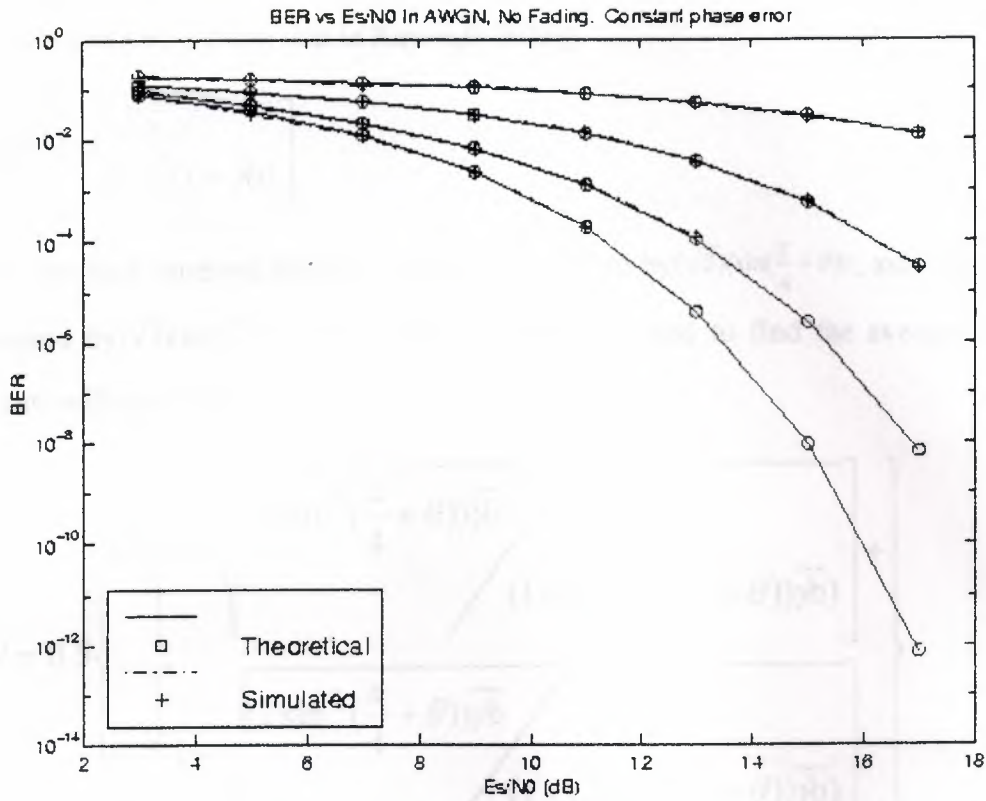


Figure 3.7 BER vs. E_s/N_0 , in AWGN and phase error.

The phase error from the top curve to the bottom curve is $3\pi/16$, $\pi/8$, $\pi/16$, and 0 radians. As a point of reference, a phase error of $\pi/4$ means that the constellation has rotated such that it is on the decision boundaries.

- In Rayleigh Fading:

The average error probability is:

$$P_b | \theta = \int P_b(\gamma_b | \theta) p(\gamma_b) d\gamma_b \quad (3.8)$$

Where $P_b(\gamma_b | \theta)$ is given by equation 3.7, and:

$$p(\gamma_b) = \frac{1}{\gamma_b} e^{-\gamma_b / \gamma_b} \quad (3.9)$$

From reference [3.9], I know that in Rayleigh fading,

$$\overline{P_b} = 0.5 \left[1 - \sqrt{\frac{\gamma \overline{b}}{1 + \gamma \overline{b}}} \right] \quad (3.10)$$

However, for each received symbol, one bit is amplified by $(\sqrt{2})(\sin(\frac{\pi}{4} + \theta))$, and the other bit is attenuated by $(\sqrt{2})(\sin(\frac{\pi}{4} - \theta))$. Therefore, when integrated to find the average gamma, these terms will carry through. So:

$$\begin{aligned} \overline{P_b} | \theta = 0.5 & \left\{ \begin{aligned} & 0.5 \left[1 - \sqrt{\frac{(2 \sin^2(\frac{\pi}{4} + \theta)) \overline{b}}{(1 + (2 \sin^2(\frac{\pi}{4} + \theta)) \overline{b})}} \right] + \\ & 0.5 \left[1 - \sqrt{\frac{(2 \sin^2(\frac{\pi}{4} - \theta)) \overline{b}}{(1 + (2 \sin^2(\frac{\pi}{4} - \theta)) \overline{b})}} \right] \end{aligned} \right\} \\ & = 0.25 \left[\begin{aligned} & 2 - \sqrt{\frac{(2 \sin^2(\frac{\pi}{4} + \theta)) \overline{b}}{(1 + (2 \sin^2(\frac{\pi}{4} + \theta)) \overline{b})}} \\ & - \sqrt{\frac{(2 \sin^2(\frac{\pi}{4} - \theta)) \overline{b}}{(1 + (2 \sin^2(\frac{\pi}{4} - \theta)) \overline{b})}} \end{aligned} \right] \quad (3.11) \end{aligned}$$

A Matlab simulation was performed to verify this. Figure 3.8 on the following page gives the results. As it can be seen in that figure, equation 3.11 agrees quite well with the simulated values. Note that QAM is much more insensitive to phase error in Rayleigh fading as compared to AWGN without fading (see figure 3.7). For phase errors less than $\pi/16$, the degradation in performance is negligible. By symmetry, a negative phase error produces the same BER as a positive phase error. Thus, only positive phase errors are shown.

Simulations below a predicted BER of 10^{-5} were not performed, due to the length of time required, as a lower BER requires a much longer sequence to produce a statistically valid result.

As a final note, this analysis does assume that the phase error is less than $\pi/4$.

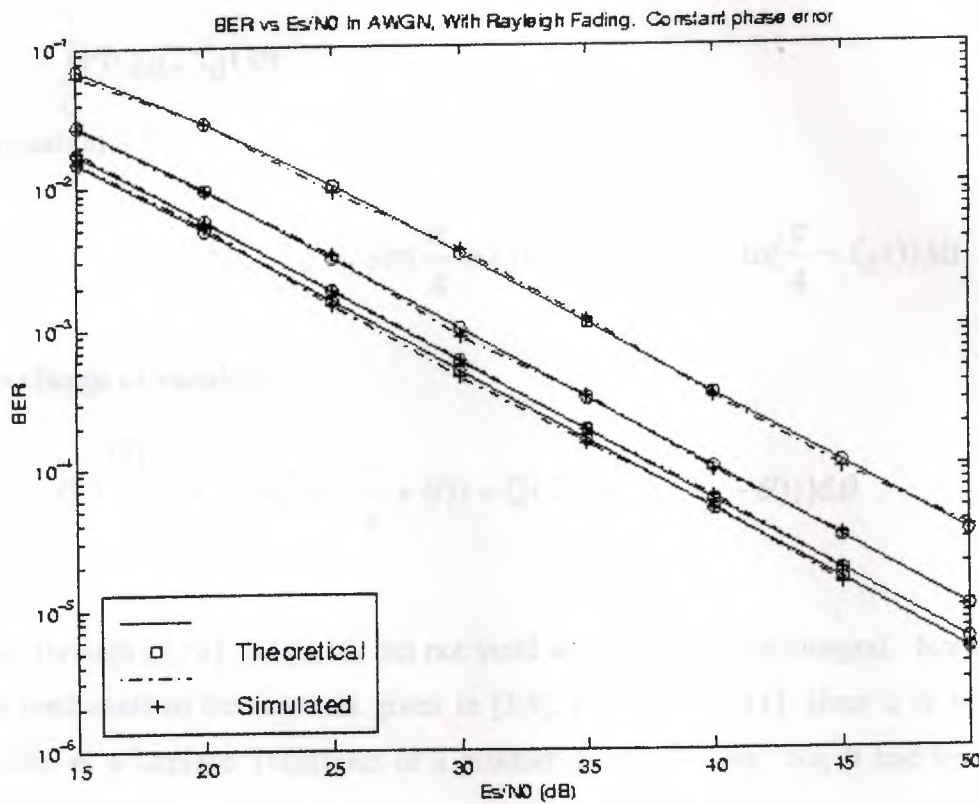


Figure 3.8 BER vs. E_s/N_0 , in AWGN with Rayleigh Fading and phase error.

The phase error from the top curve to the bottom curve is $3\pi/16$, $\pi/8$, $\pi/16$, and 0 radians. As a point of reference, a phase error of $\pi/4$ means that the constellation has rotated such that it is on the decision boundaries.

3.4.2 Constant Doppler (Frequency Offset) Error

- In AWGN:

To model the effects of Doppler error, It has been assumed that the frequency shift could be modeled as a phase ramp, such that:

$$\theta(t) = 2\pi f_d t \quad (3.12)$$

Where f_d is the frequency deviation from the actual carrier frequency. Additionally, for this analysis, It had been assumed that the initial phase error is zero. Therefore,

$$P_b | f_d = \int_0^T P_b | (\theta = f_d t) dt \quad (3.13)$$

Using equation 3.7:

$$P_b | f_d = 0.5 \int_0^T \{Q(2\sqrt{\gamma_b} \sin(\frac{\pi}{4} + f_d t)) + Q(2\sqrt{\gamma_b} \sin(\frac{\pi}{4} - f_d t))\} dt \quad (3.14)$$

Or, by a change of variables:

$$P_b | f_d = 0.5 \int_0^{fdT} \{Q(2\sqrt{\gamma_b} \sin(\frac{\pi}{4} + \theta)) + Q(2\sqrt{\gamma_b} \sin(\frac{\pi}{4} - \theta))\} d\theta \quad (3.15)$$

A search through [3.13] and [3.14] did not yield any help with this integral. Nor does this integral lend itself to the methods given in [3.9], [3.10], or [3.11], since it is not readily expressible as a Laplace Transform or a product of expressions. So, It had been solved numerically.

A Mat lab simulation was performed to verify equation 3.15. Figure 3 9on the following page gives the results. As can be seen in that figure, equation 15 agrees quite well with the simulated values. Again, QAM is relatively sensitive to frequency deviation in AWGN, just as it was sensitive to phase error in AWGN. Different values for f_d and T were tried. The results only depended on the product $f_d T$, as equation 3.15 predicts.

As a final note, this analysis does assume that the product $f_d T$ is less than $\pi/4$.

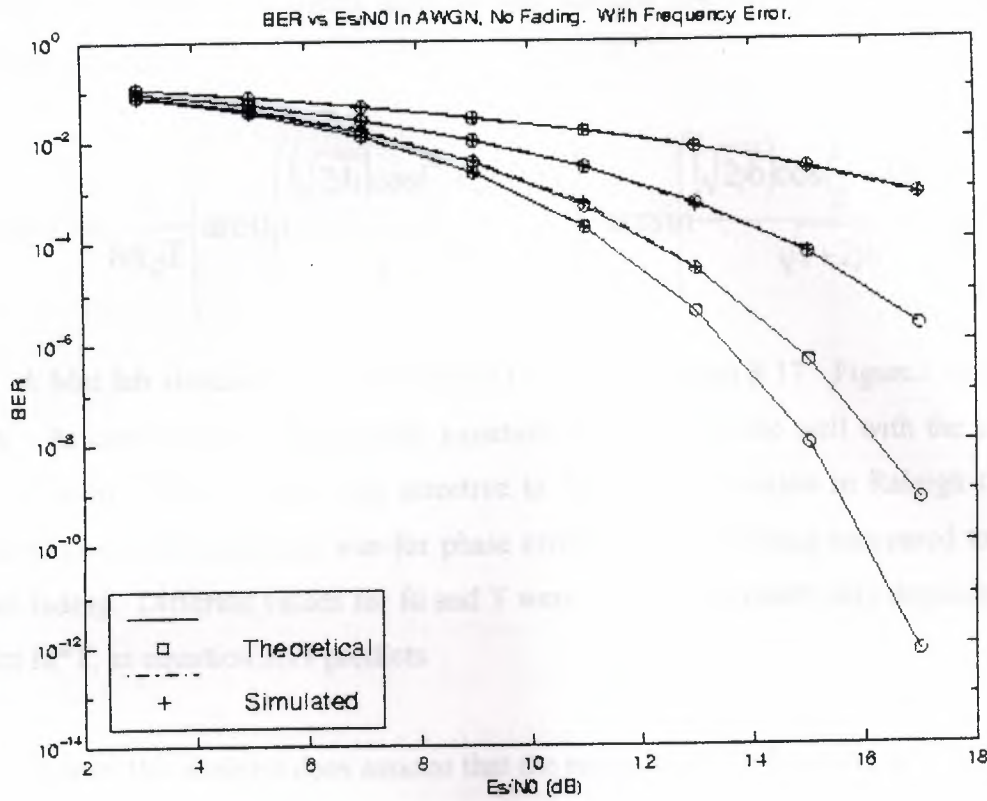


Figure 3.9 BER vs. E_s/N_0 , in AWGN with frequency error.

$fd \cdot T$ from the top curve to the bottom curve is $3\pi/16$, $\pi/8$, $\pi/16$, and π radians.

- In Rayleigh:

Again, the phase ramp method was used to analyze the effects of frequency deviation in Rayleigh fading. Again, the initial phase offset is assumed to be zero. Plugging equation 3.13 into equation 3.11 yields:

$$\overline{P_b} |_{fd = 0.25} \int_0^{fdT} \left[\frac{2 - \sqrt{\frac{(2 \sin^2(\frac{\pi}{4} + \theta)) \overline{\gamma b}}{(1 + (2 \sin^2(\frac{\pi}{4} + \theta)) \overline{\gamma b})}}}{- \sqrt{\frac{(2 \sin^2(\frac{\pi}{4} + \theta)) \overline{\gamma b}}{(1 + (2 \sin^2(\frac{\pi}{4} + \theta)) \overline{\gamma b})}}} \right] d\theta \quad (3.16)$$

Fortunately, reference 3.14 offers help for this integral sparing all of the mathematical details, the result is:

$$\overline{P_b}|_{fd=0.5} = 0.5 + \frac{1}{8\pi f_d T} \left\{ \arcsin \left(\frac{\left(\sqrt{2\gamma_b} \right) \cos\left(\frac{\pi}{4} + 2\pi f_d T\right)}{\sqrt{1+2\gamma_b}} \right) - \arcsin \left(\frac{\left(\sqrt{2\gamma_b} \right) \cos\left(\frac{\pi}{4} - 2\pi f_d T\right)}{\sqrt{1+2\gamma_b}} \right) \right\} \quad (3.17)$$

A Mat lab simulation was performed to verify equation 3.17. Figure 3.10 gives the results. As can be seen in that figure, equation 3.17 agrees quite well with the simulated values. Again, QAM is much less sensitive to frequency deviation in Rayleigh fading as compared to AWGN, just as it was for phase error in Rayleigh fading compared to AWGN without fading. Different values for f_d and T were tried. The results only depended on the product $f_d T$, as equation 3.17 predicts.

As a final note, this analysis does assume that the product $f_d T$ is less than $\pi/4$.

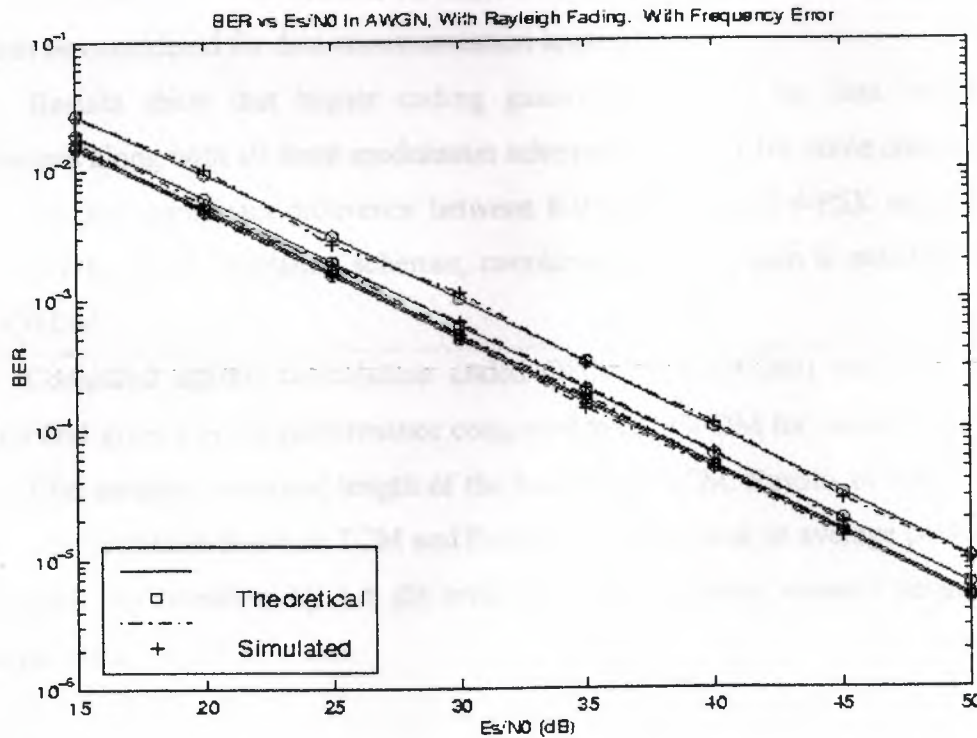


Figure 3.10 BER vs. E_s/N_0 , in AWGN with frequency error.

Table3. 2 PAPR with and without PTS for different modulation schemes with and without TCM

Modulation Scheme	PAPR with PTS and without coding	PAPR without PTS and without coding	PAPR with PTS and with coding	PAPR without PTS and with coding
8-PSK	6.74 dB	8.16 dB	6.97 dB	8.35 dB
16-QAM	6.72 dB	8.41 dB	6.88 dB	8.37 dB
32-QAM	6.72 dB	8.35 dB	6.89 dB	8.05 dB

3.7 TCM-OFDM

In this regard, different modulation techniques are considered with TCM-OFDM for a Rician fading channel. Rectangular (16-QAM, 32-QAM) and circular (8-PSK) constellation modulation schemes are considered with trellis coded modulation. Coding gain is considered at two different values of BER. These two levels of BER are selected because BER of 10^{-2} is considered for most of the voice communication applications and 10^{-4} can be considered for data communication applications.

Results show that higher coding gains are possible for data communication applications along with all three modulation schemes. However for voice communications, there is no any significant difference between 8-PSK coded and 4-PSK encoded system. But, with other two modulation schemes, considerable coding gain is possible. Results of TCM-OFDM

Compared against convolution coded OFDM (CC-OFDM) and it is found that TCMOFDM gives a better performance compared to CC-OFDM for reduced complexity in terms of the smaller constraint length of the encoder in TCM. Results of PAPR show that there is no correlation between TCM and PAPR. However, Peak to average power ratio can be reduced approximately by 1.6 dB with the help of partial transmit sequence (PTS) technique even with TCM.

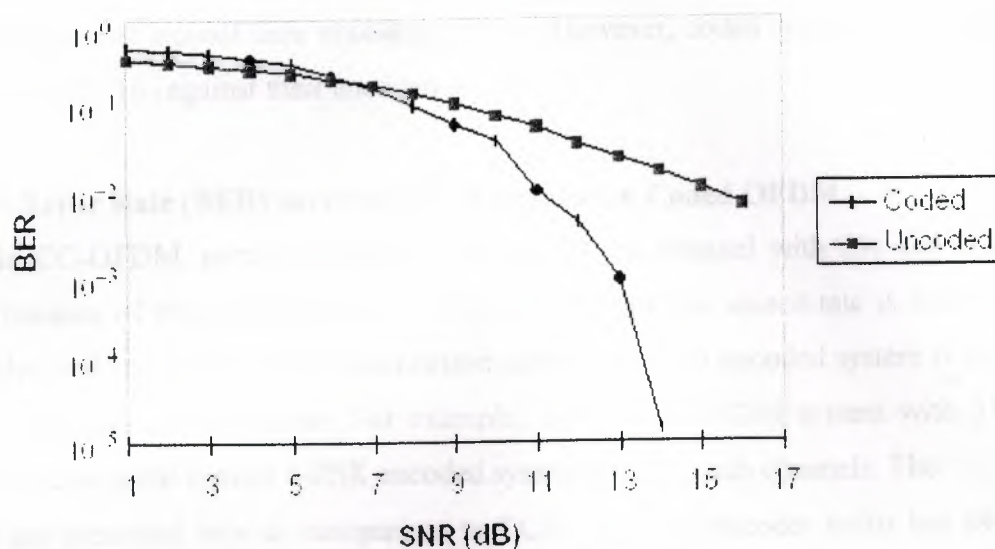


Figure 3.18 BER performance for 16-QAM

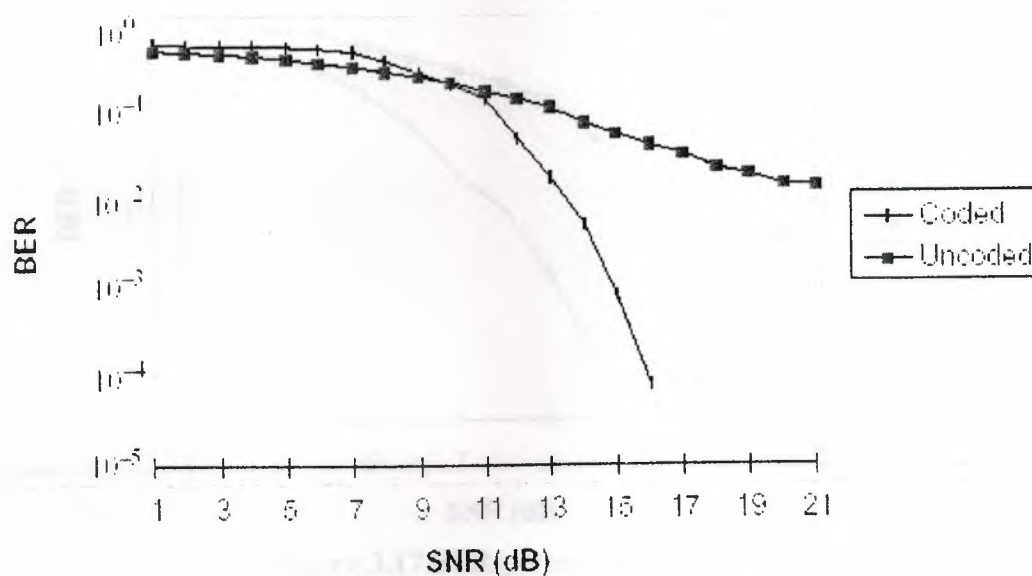


Figure 3.19 BER performance for 32-QAM

3.6 Peak to Average Power Ratio

Table 3.2 shows the PAPR for three different modulation schemes. It shows that TCM doesn't have any significant influence on PAPR. PTS can reduce PAPR by 1.6 dB with coding.

there is not much significant difference between coded 8-PSK system and encoded 4-PSK system performance. But, for 16-QAM and 32-QAM systems coded system give the better performance against their encoded systems. However, coded systems are much more superior at BER 10^{-4} against their encoded system.

3.5.2 Bit Error Rate (BER) performance: Convolution Coded OFDM

In CC-OFDM, encoded system is defined as the channel with 256 sub channels. This is because of the coding rate is $\frac{1}{2}$. This ensures that the source rate is fixed against both coded and encoded systems. Modulation scheme for each encoded system is the same as the respective coded scheme. For example, 8-PSK CC-OFDM system with 512 sub channels is compared against 8-PSK encoded system with 256 sub channels. The Results are presented here as comparison to TCM. Here the encoder trellis has 64 states whereas in the TCM case it is only 8.

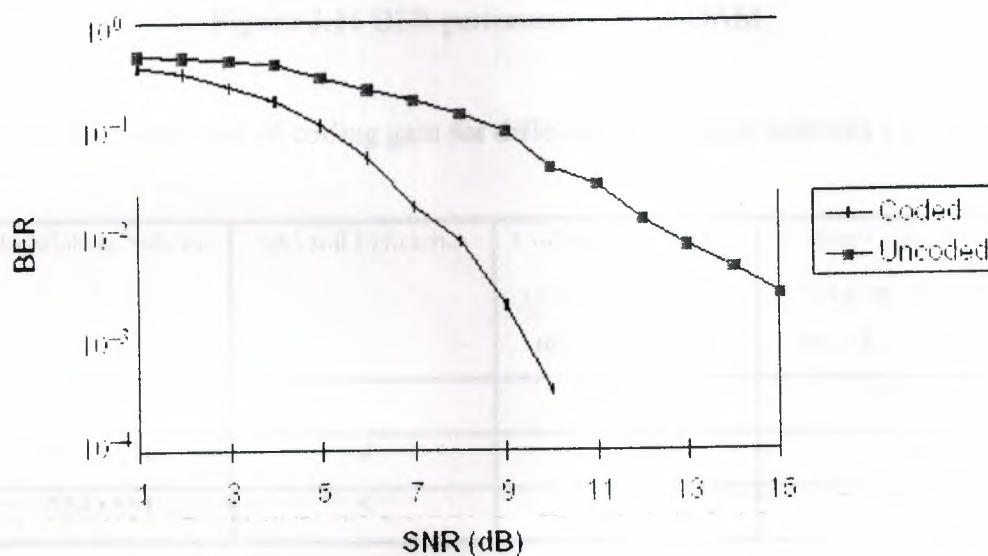


Figure 3.17 BER performance for 8-PSK

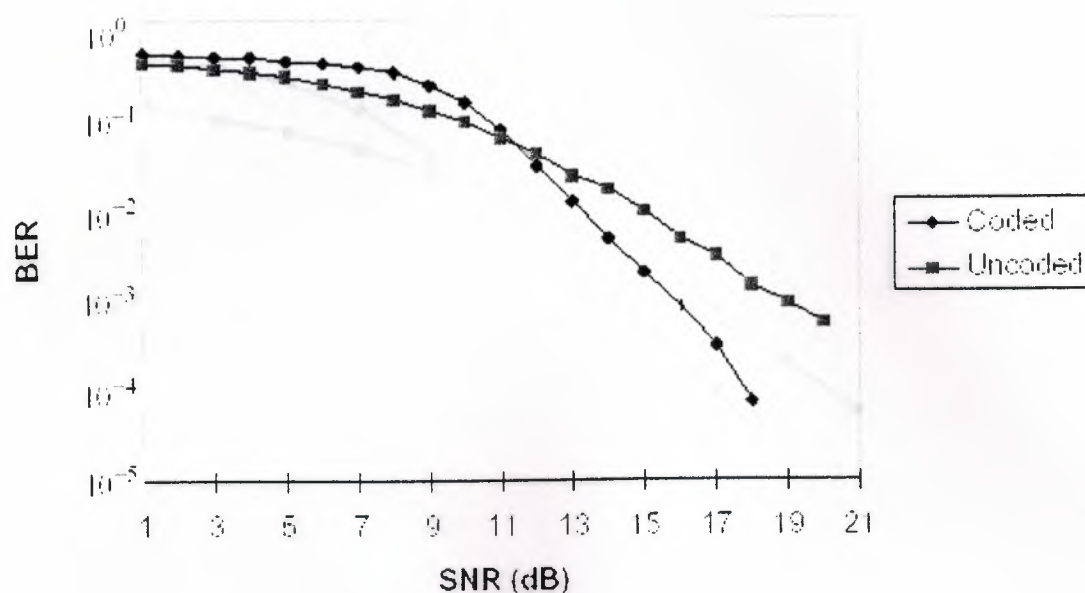


Figure 3.16 BER performance of 32-QAM

Table 3.1 Comparison of coding gain for different modulation schemes (L Band)

Modulation Scheme	Spectral Efficiency	Coding Gain at 10^{-2} over conventional uncoded system	Coding Gain at 10^{-4} over conventional uncoded system
8-PSK	3	0.1 dB	1.5 dB
16-QAM	4	2.2 dB	4.0 dB
32-QAM	5	1.8 dB	2.0 dB

Coding gain is analyzed at BER of 10^{-2} and 10^{-4} . BER of 10^{-2} is considered for voice applications whereas 10^{-4} is considered for data applications. Summarized results (Table 3.1) show that high coding gain is possible for higher modulation schemes. During the simulations, BER performances of several configurations of 8-state encoder model are analyzed. It has been found that Unger boeck encoders [3.17] for fading channels give the best performance for OFDM as well. It should be noted that for voice communications,

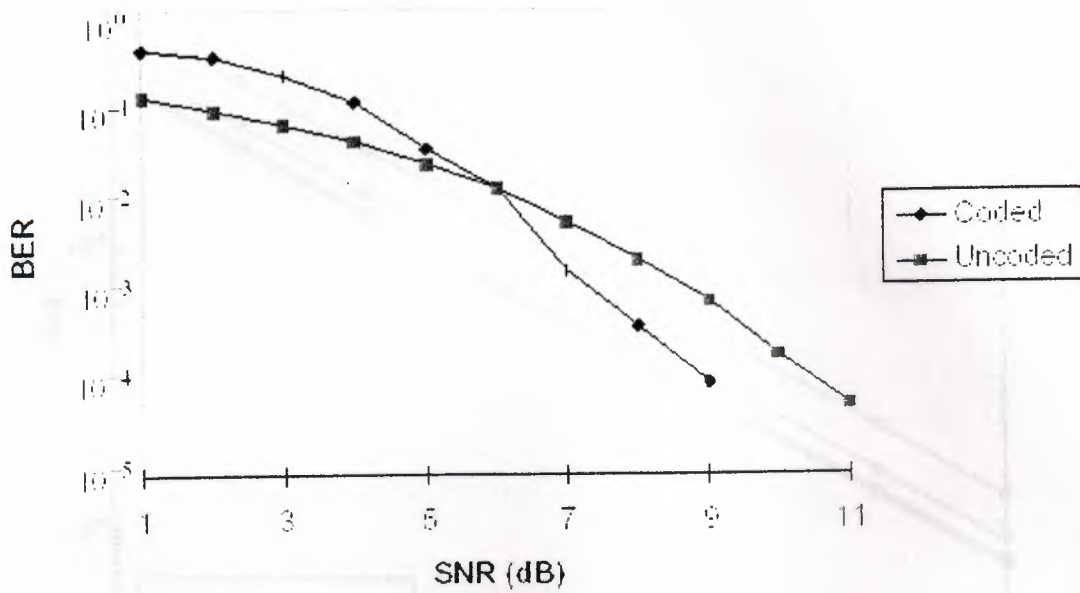


Figure 3.14 BER performance of 8-PSK

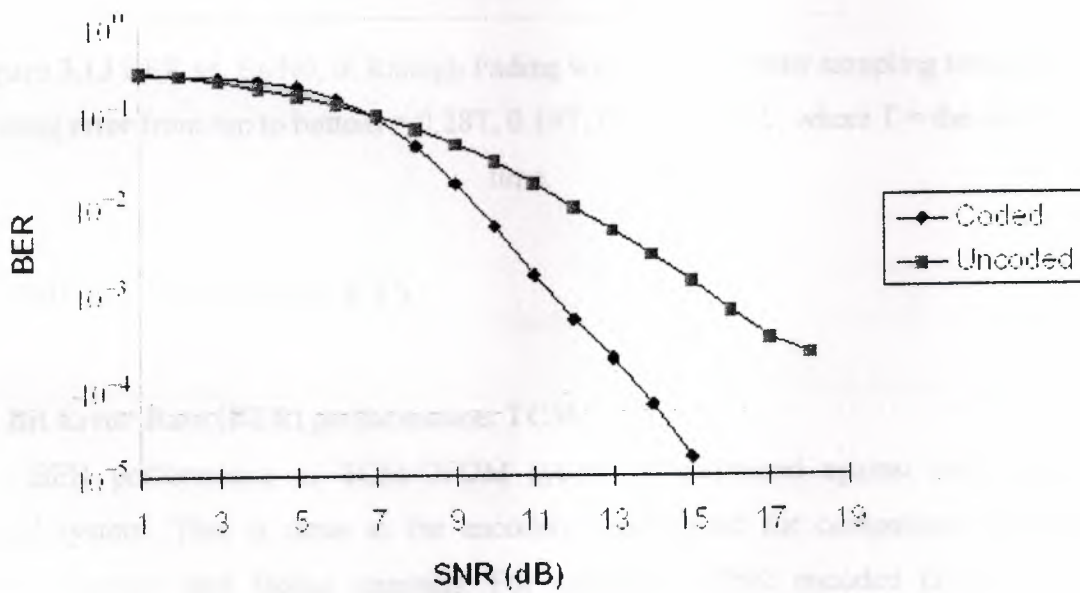


Figure 3.15 BER performance of 16-QAM

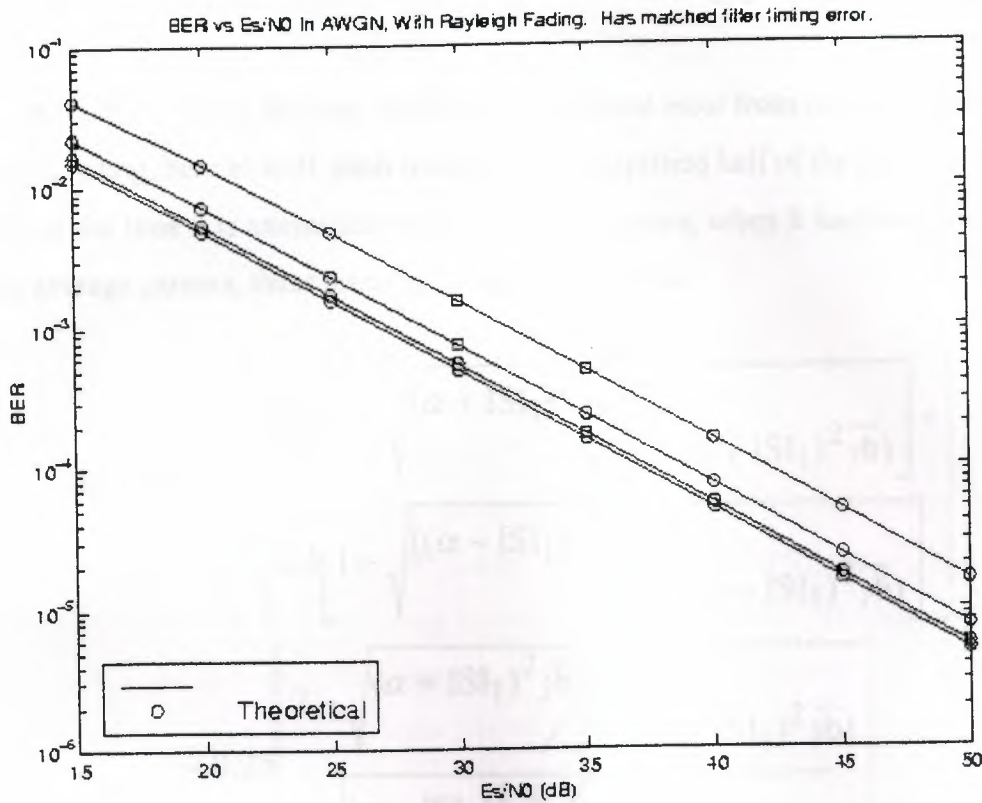


Figure 3.13 BER vs. E_s/N_0 , in Rayleigh Fading with matched filter sampling time error. Timing error from top to bottom = $0.28T$, $0.19T$, $0.094T$, and 0 , where T = the symbol time.

3.5 SIMULATION RESULTS

3.5.1 Bit Error Rate (BER) performance: TCM

BER performance of TCM-OFDM system is compared against its respective encoded system. This is same as the encoded system used for comparison [3.17] for AWGN channels and fading channels. For example, 8-PSK encoded OFDM is the conventional encoded system for 16-QAM TCM-OFDM system. Similarly for 8-PSK TCM-OFDM system 4-PSK is the encoded system and for 32-QAM TCM-OFDM system, 16-QAM encoded system is considered as the uncoded scheme. For all uncoded systems, the number of subchannels is also same as the coded system. BER curves are compared with this argument.

Timing error from top to bottom = $0.28T$, $0.19T$, $0.094T$, and 0 , where T = the symbol time.

In Raleigh Fading the case when extending phase error from AWGN without fading to Raleigh fading, here as well, each received bit is amplified half of the time by $(\alpha + ISI_1)$, and half of the time it is attenuated by $(\alpha - ISI_1)$. Therefore, when It had been integrated to find the average gamma, these terms will carry through. So:

$$\begin{aligned} \overline{P_b} | ISI = 0.5 &= \left\{ 0.5 \left[1 - \sqrt{\frac{(\alpha + ISI_1)^2 \overline{\gamma b}}{1 + (\alpha + ISI_1)^2 \overline{\gamma b}}} \right] + \right. \\ &\quad \left. 0.5 \left[1 - \sqrt{\frac{(\alpha - ISI_1)^2 \overline{\gamma b}}{1 + (\alpha - ISI_1)^2 \overline{\gamma b}}} \right] \right\} \\ &= 0.25 \left[2 - \sqrt{\frac{(\alpha + ISI_1)^2 \overline{\gamma b}}{1 + (\alpha + ISI_1)^2 \overline{\gamma b}}} \right. \\ &\quad \left. - \sqrt{\frac{(\alpha - ISI_1)^2 \overline{\gamma b}}{1 + (\alpha - ISI_1)^2 \overline{\gamma b}}} \right] \end{aligned} \quad (3.20)$$

The above analysis does assume slow fading, since it is assumed that ISI from symbols further away from the desired symbol remain deeply attenuated after matched filtering.

Simulation code was written to verify 3.20. . This is shown in Figure 3.11.

- + Probability that the dominant interfering bit is of different value than the desired bit
- x Probability that $(\alpha - ISI_1) > \text{noise}$

$$\begin{aligned}
 P_b &= 0.5Q\left(\frac{(\alpha + ISI_1)\sqrt{Eb}}{\sqrt{N_0/2}}\right) + 0.5Q\left(\frac{(\alpha - ISI_1)\sqrt{Eb}}{\sqrt{N_0/2}}\right) \\
 &= 0.5\left\{Q\left((\alpha + ISI_1)\sqrt{\gamma_b}\right) + Q\left((\alpha - ISI_1)\sqrt{\gamma_b}\right)\right\}
 \end{aligned}
 \tag{3.19}$$

A Mat lab simulation was performed to verify equation 3.19. Figure 3.10 on the following page gives the results. It can be seen in that figure, equation 3.19 agrees reasonably well with the simulations. There is a slight deviation for the lower BER tests. It is unfortunate that these simulations take a very long time to run, as it makes exploring this deviation difficult. However, a potential refinement to equation 19 is to model the remaining ISI terms as Gaussian noise, and thus they would add to the denominator terms in the Q-functions of equation 3.19.

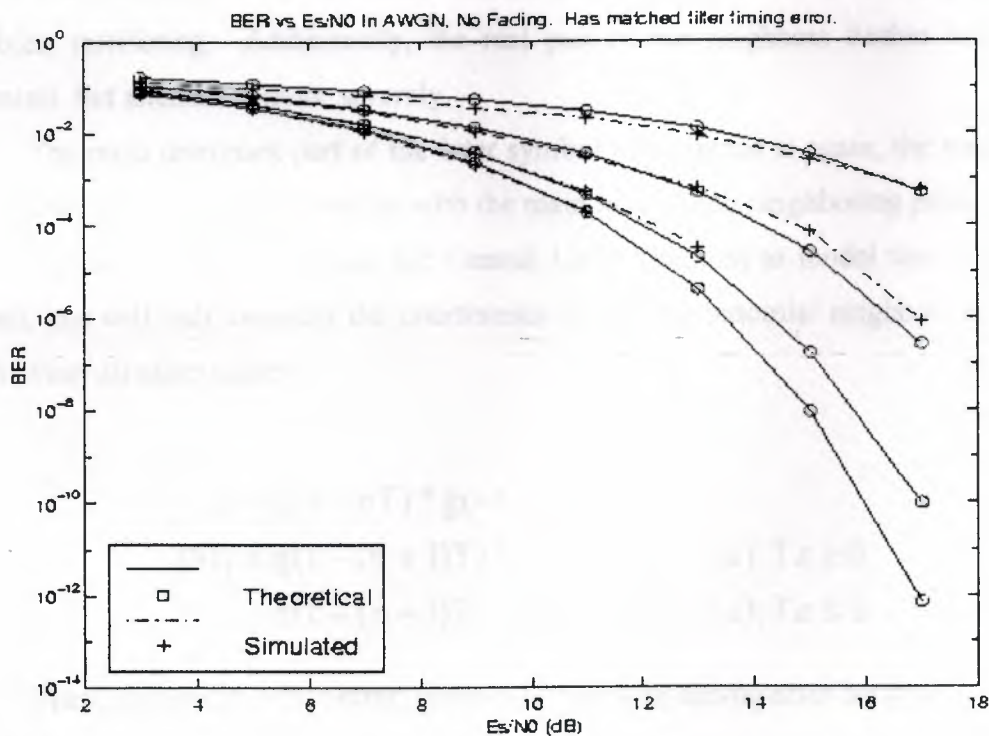


Figure 3.12 BER vs. E_s/N_0 , in AWGN with matched filter sampling time error.

$$r(n) = d(n)g(t - nT) * g(-t + nT + T\varepsilon) + \sum_{k \neq n} (d(k)g(t - kT) * g(-t + nT + T\varepsilon)) + n(t) * g(-t + nT + T\varepsilon) \quad (3.18)$$

Where the first term on the right hand side represents the desired signal, the second summation term represents inter symbol interference, and the third term represents noise. The symbols and the noise are complex values. Assuming that my matched filter is orthonormal, and that $n(t)$ is complex Gaussian noise, the third term after convolution will have the same variance as the original noise.

- In AWGN:

To model the inter symbol interference over all of the interfering terms would be rather protracted. There will be the dominant main lobe of the matched filter that overlaps further and further with the main lobe of a nearest neighboring pulse. Also, the matched filter will absorb energy (to a lesser extent) from pulses in the vicinity. Therefore, the real part of the interference has dominant nearest neighboring symbols, which are binomial variables, interfering. Additionally, the real part of the neighbors further out are also binomials, but attenuated more severely.

The most dominant part of the inter symbol interference is again, the main lobe of the matched filter starting to overlap with the main lobe of one neighboring pulse. Because of this dominance, it has invoked the Central Limit Theorem to model this interference. Instead, this will only consider the interference if this one binomial neighbor, and neglect the ISI from all other pulses.

Let

$$\begin{aligned} \alpha &= g(t - nT) * g(-t + nT + T\varepsilon) \\ ISI_1 &= g(t - (n + 1)T) * g(-t + nT + T\varepsilon); T\varepsilon \geq 0 \\ &= g(t - (n - 1)T) * g(-t + nT + T\varepsilon); T\varepsilon \leq 0 \end{aligned}$$

Then, probability of bit error, given matched filter timing error becomes:

P_b = Probability that the dominant interfering bit is the same value as the desired bit
 x Probability that $(\alpha + ISI_1 > \text{noise})$

$fd \cdot T$ from the top curve to the bottom curve is $3\pi/16$, $\pi/8$, $\pi/16$, and π radians.

As a final note, the results for Doppler error can be extended to a non-zero initial phase simply by adding in or subtracting out a weighted sum of equations 3.15, 3.17. For example, if the initial phase is θ , one can calculate relationship 3.15, 3.17 from 0 to θ , and from 0 to the final $fd \cdot T$. Then, a weighted subtraction of the two values will give the predicted error.

3.4.3 Constant Pulse Timing Error

The concerned about a timing error in sampling the matched filter of the receiver We assuming a Root Cosine Pulse. This has the following amplitude response:

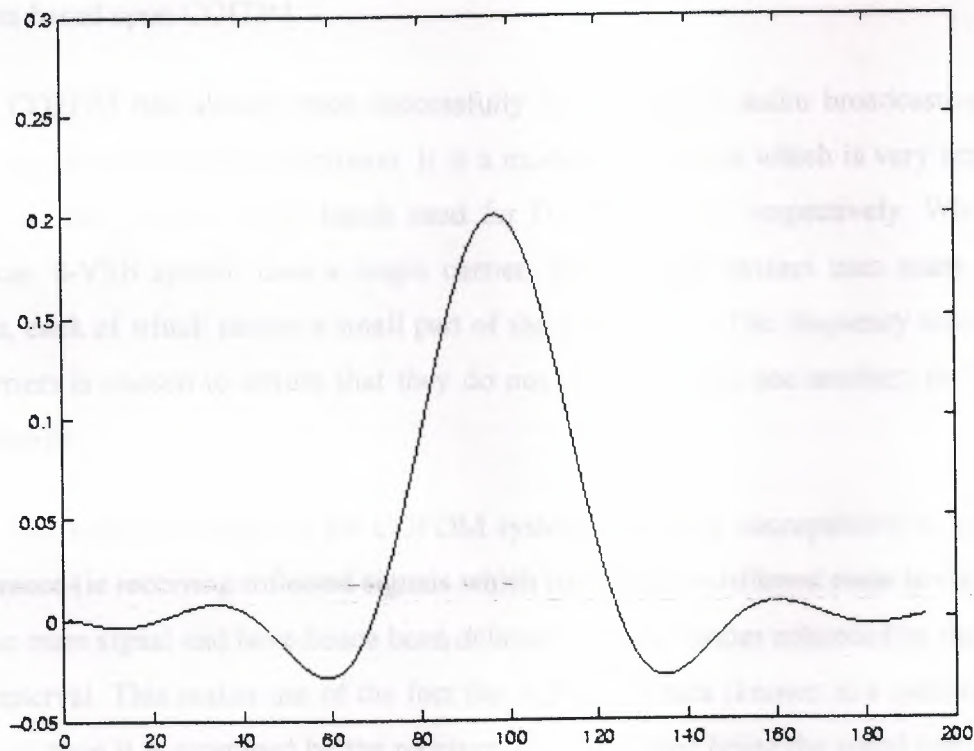


Figure 3.11 FIR of a Root Raised Cosine Pulse, 32 samples per symbol period T , duration = 6 symbol periods, = $6T$

Assuming the matched filter is sampled at time $nT + T\epsilon$, where $T\epsilon$ represents a sampling timing error, the sampled detection statistic is:

4. DIGITAL VIDEO BROADCASTING

4.1 Coded Orthogonal Frequency Division Multiplexing (COFDM)

The drive to deliver increased radiofrequency spectrum utilization, robust Immunity from noise and interference, and wider operating range led to the adoption of Coded Orthogonal Frequency Division Multiplexing (COFDM) by the European Telecommunications Standards Institute (ETSI) for Digital Video Terrestrial Broadcasting (DVB-T) and Digital Audio Broadcasting (DAB).

Originally used by the military for secure radio transmissions, the recent availability of fast, inexpensive digital signal processing chips has led many companies to develop products based upon COFDM.

COFDM had already been successfully used in digital audio broadcasting (DAB) before the advent of digital television. It is a modulation system which is very appropriate for use in the VHF and UHF bands used for DAB and DTV respectively. Whereas the American 8-VSB system uses a single carrier, the COFDM system uses many separate carriers, each of which carries a small part of the overall data. The frequency separation of the carriers is chosen to ensure that they do not crosstalk with one another, ie they have orthogonally.

The main advantage of the COFDM system is the low susceptibility to multi path interference (ie receiving reflected signals which have taken a different route to the receiver than the main signal and have hence been delayed). This is further enhanced by the use of a guard interval. This makes use of the fact that a block of data (known as a symbol) is sent for longer than it is examined by the receiver, this extra time being the guard interval. This guard interval may be chosen based on the expected multi path signals of the particular system.

If this interval is chosen carefully it can also lead to the use of single frequency networks, which make use of the fact that a delayed signal from a far transmitter will appear as a multi path signal, ignored in the guard interval. The other way in which the

effect of multi path interference (and also interference from co-channel analogue TV signals) is reduced is by careful coding of the data such that there is sufficient extra data encoded to allow corrupt data to be corrected in the receiver. The COFDM signal itself will not greatly interfere with analogue channels since it is transmitted at a low power (due to a very low signal to noise ratio) and it has a similar characteristic to flat noise.

4.2 Data Rates using QAM and QPSK

The characteristics of the COFDM system can be varied to optimize the systems performance with different modulation schemes. While the most robust is QPSK, it has the limitation of only being able to achieve data rate of 10.6 Mbps. The table below shows more practical systems.

Table 4.1 Data rates of QAM

Modulation	Code Rate	Failure Point	Data Rate
16 QAM	1/2	12 dB	12 Mbps
32 QAM	3/4	16.5 dB	18 Mbps
64 QAM	2/3	20 dB	24 Mbps

Therefore, while the 64-QAM has a superior data rate, it is liable to fail before the other systems. Coverage using this system is therefore reduced in order to achieve the higher data rate.

4.3 DVB standards

The satellite version of digital video broadcasting (DVB-S), is almost universally adopted. Digital TV transmissions are possible in five continents via satellite. These broadcastings have already begun at least in some European countries, northern America and in Australia. The DVB-T has also gained a lot of popularity in many countries. Japan

and the United States have developed own standards in addition to DVB-S. Worldwide standards appear to be an impossible idea. It seems that three main areas Europe, Japan and USA can not agree on anything.

4.3.1 DVB-S

DVB-S is designed to cope the full range of satellite transmissions. It is the oldest and the most established of the DVB standards. All data is first inserted into fixed-length MPEG transport stream packets. The data is then formed into a regular structure and contents are randomized Reed-Solomon Forward Error-Correction (FEC) overhead is added to data. After FEC, convolution aligner leaving is applied followed by further error-correction in a form of punctured convolution code. Finally a single carrier-wave is modulated using quadrature phase-shift keying (QPSK).

An example system has a 36 MHz bandwidth available. If 3/4 convolution code is utilized, useful bit rate of about 39 Mbit/s will be available. Thus, system can be used to transmit any combination of MPEG-2 video and audio.

4.3.2 DVB-C

The DVB-C is based directly on DVB-S. The modulation scheme used is quadrature amplitude modulation (QAM), instead of QPSK. The basic method is 64-QAM but lower-level systems (16- and 32-QAM) and higher-level systems (128- and 256-QAM) are also possible. Alternative systems allow trade-offs between system capacity and complexity. Forward error correction is not needed in cable networks. The capacity of 38.5 Mbit/s is achievable with 64-QAM if 8 MHz channel bandwidth is available. The cable network system, known as DVB-C, has the same core properties as the satellite system, but the modulation is based on quadrature amplitude modulation (QAM) rather than QPSK, and no inner-code forward error correction is used. The system is centered on 64-QAM, but lower-level systems, such as 16-QAM and 32-QAM, also can be used. In each case, the data capacity of the system is traded against robustness of the data.

Higher-level systems, such as 128-QAM and 256-QAM, also may become possible, but their use will depend on the capacity of the cable network to cope with the reduced

decoding margin. In terms of capacity, an 8 MHz channel can accommodate a payload capacity of 38.5 Mbits/s if 64-QAM is used, without spillover into adjacent channels.

4.3.3 DVB-T

DVB-T is the system specification for the terrestrial broadcasting of digital television signals. DVB-T was approved by the DVB Steering Board in December 1995. This work was based on a set of user requirements produced by the Terrestrial Commercial Module of the DVB project. DVB members contributed to the technical development of DVB-Through the DTTV-SA (Digital Terrestrial Television—Systems Aspects) of the Technical Module. The European Projects SPECTRE, STERNE, HD-DIVINE, HDTV, dTTb, and several other organizations developed system hardware and produced test results that were fed back to DTTV-SA.

As with the other DVB standards, MPEG-2 audio and video coding forms the payload of DVB-T. Other elements of the specification include

- A transmission scheme based on orthogonal frequency-division multiplexing (OFDM), which allows for the use of either 1705 carriers (usually known as 2k), or 6817 carriers (8k). Concatenated error correction is used. The 2k mode is suitable for single-transmitter operation and for relatively small single-frequency networks with limited transmitter power. The 8k mode can be used both for single-transmitter operation and for large-area single-frequency networks. The guard interval is selectable.
- Reed-Solomon outer coding and outer convolution interleaving are used, as with the other DVB standards.
- The inner coding (punctured convolution code) is the same as that used for DVB-S.
- The data carriers in the coded orthogonal frequency-division multiplexing (COFDM) frame can use QPSK and different levels of QAM modulation and code rates to trade bits for ruggedness.
- Two-level hierarchical channel coding and modulation can be used, but hierarchical source coding is not used.

The latter was deemed unnecessary by the DVB group because its benefits did not justify the extra receiver complexity that was involved.

4.3.4 DVB-MS

The DVB-MS digital multipoint distribution system uses microwave frequencies above approximately 10 GHz for direct distribution to viewers' homes [3]. Because this system is based on the DVB-S satellite delivery system, DVB-MS signals can be received by DVB-S satellite receivers. The receiver must be equipped with a small microwave multipoint distribution system (MMDS) frequency converter, rather than a satellite dish.

4.4 Processing of DVB-S

DVB-S is a satellite-based delivery system designed to operate within a range of transponder bandwidths (26 to 72 MHz) accommodated by European satellites such as the Strategies, Outlast series, Hippest, Telecom series, Tele-X, Thor, TDF-1 and 2, and DFS. DVB-S is a single carrier system, with the *payload* (the most important data) at its core. Surrounding this core is a series of layers intended not only to make the signal less sensitive to errors, but also to arrange the payload in a form suitable for broadcasting. The video, audio, and other data are inserted into fixed-length MPEG transport-stream packets. This packetized data constitutes the payload.

A number of processing stages follow:

- The data is formed into a regular structure by inverting synchronization bytes every eighth packet header.
- The contents are randomized.
- Reed-Solomon forward error correction (FEC) overhead is added to the packet data. This efficient system, which adds less than 12 percent overhead to the signal, is known as the outer code. All delivery systems have a common outer code.
- Convolution interleaving is applied to the packet contents.
- Another error-correction system, which uses a punctured convolution *code*, is added.

This second error-correction system, the inner code, can be adjusted (in the amount of overhead) to suit the needs of the service provider.

- The signal modulates the satellite broadcast carrier using quadrature phase-shift keying (QPSK).

In essence, between the multiplexing and the physical transmission, the system is tailored to the specific channel properties. The system is arranged to adapt to the error

characteristics the channel. Burst errors are randomized, and two layers of forward error correction are added. The second level (inner code) can be adjusted to suit the operational circumstances (power, dish size, bit rate available, and other parameters).

4.5 ITU Modem Standards

ITU modem can be classified into two groups: Those are essentially equivalent to Bell series and those that are not. Some common modulation Standard are given in

Table 4.1 ITU /Bell compatible

ITU	BELL	Bit rate	Modulation
V.21	103	300	FSK
V.22	212	1200	4-PSK
V.23	202	1200	FSK
V.26	201	2400	4-PSK
V.27	208	4800	8-PSK
V.29	209	9600	16-QAM

The ITU modems that do not have equivalents in the bell series are given in Table 4.2

4.5 .1 ITU Modems V.22bis

ITU V.22bis specification provides for 1200 and 2400-bps Synchronous HDX communication over switched and two –wire leased lines. Four phase DPSK is employed as the modulation technique for modem operation at 1200 bps. QAM is used to achieve the data transfer rate 2400 bps .Modulation rate is specified at 600 baud for both operating speeds . Full Duplex operation is achieved by phase and amplitude shift keying a low channel carrier frequency of 1200 Hz and high channel carrier frequency of 2400 Hz.

4.5.2 V.32bis Standard

For example, the V.32bis standard is for modems operating at a maximum rate of 14.4 Kbps using a 2400 symbols per sec. signaling rate (baud rate). This standard is based on a QAM constellation of size 128, with 6 data bits transmitted with each symbol ($6 \times 2400 = 14400$). The 128-point QAM Constellation is essentially a square 12×12 constellation with 4 points Removed at each corner and the whole rotated by 45 deg.

The extra bit Redundancy available in the constellation ($128=2^7$) is exploited to build-in Error correction, The bandwidth efficiency of this modem is $14400/3000 = 4.8$ bits/Hz With approximately 3.1 KHz of transmission bandwidth (300 to 3400 Hz), the baud rate of 2400 implies that each pulse (of duration roughly $1/2400$ sec) has a bandwidth of roughly 1500 Hz, a little above that implied by the Nyquist limit (1200 Hz).

The pulses have a fairly carefully chosen shape. These modems operate in full duplex mode; this is achieved over the two wire (single wire-pair) telephone line by employing hybrid transformers and echo cancellers.

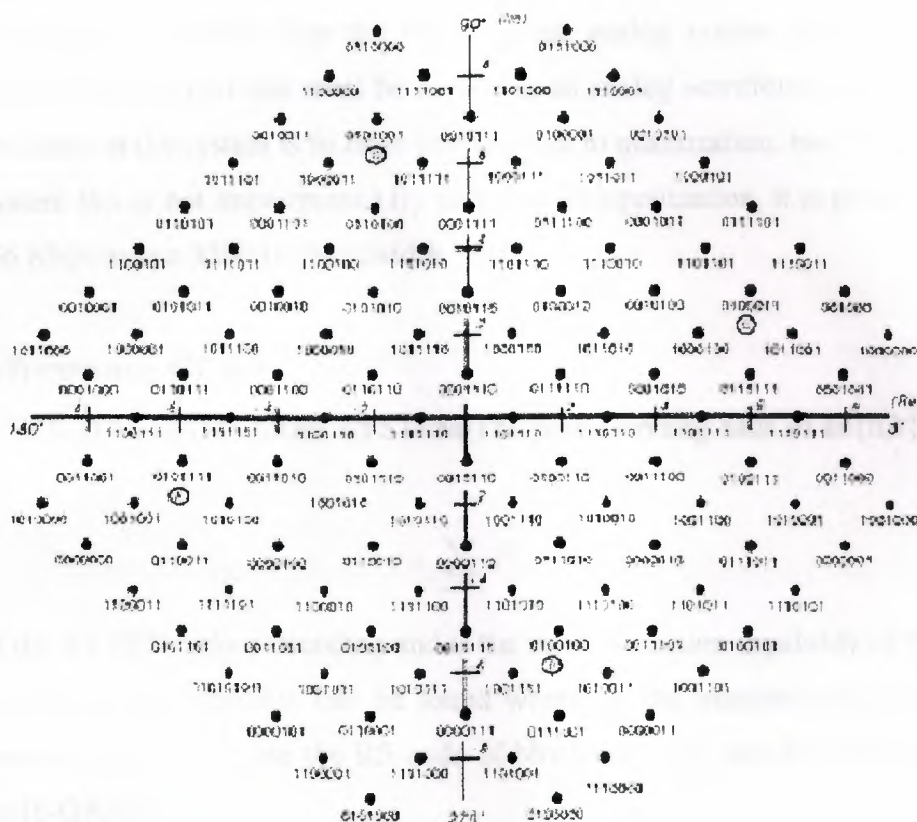


Figure 4.1 128-Points QAM Constellation Used in a V.32bis Modem

4.5.3 V.34 and V.34bis Standard

A more recent modem standard (V.34) specifies a full-duplex data rate of 28.8 Kbps, and V.34bis includes specifications for a top data rate of 33.6 Kbps. These standards allow for various symbol and data rates, depending on channel conditions. For example, a constellation size of 768 with a symbol rate of 3200 baud and 9 data bits per symbol (with redundancy in the constellation for coding) gives a 28.8 Kbps data rate.

Note that here the minimum theoretical bandwidth required is 3200 Hz (Nyquist limit) for the amplitude/phase modulated pulse stream at 3200 Baud. Thus very good equalization and pulse shaping has to be incorporated. These modems use rather sophisticated error control coding to provide reliable data transmission. We shall discuss simple error control coding schemes later on. The most recent modems for data transmission over the PSTN are the 56 Kbps modems. It would appear that this rate is in

violation of the Shannon limit, given the bandwidth and the SNR for the line! However, these modems exploit the fact that the PSTN for the most part uses digital techniques, whereas the other modems view the PSTN as the analog system that it was originally designed as. The only part that must be viewed as an analog waveform channel is the local loop. The noise in the system is in large part that due to quantization, but in the digital view of the system this is not impairment.) By very careful equalization, it is possible to receive data at 56 Kbps over a 3500 Hz bandwidth.

4.6 Performance Of RS

CODED 16-QAM OFDM SYSTEM The post decoding SER of an $\{n,k\}$ RS code is given by

$$P_{b,n} = \sum_{i=0}^n P_{b,i} \binom{n}{i} (1 - P_{b,i})^{n-i}$$

where $P_{b,i}$ is the RS SER before decoding and i is the error correction capability of the RS code. The error correction capability can be found where, as the numbers of sub carriers and guard samples vary. If we use the RS code of block size 255, one RS symbol is mapped onto two 16-QAM.

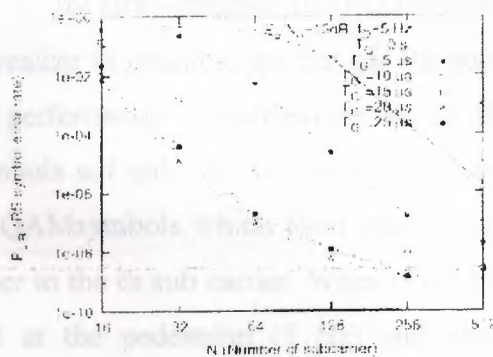


Fig. 4.2. RS SER versus N when $f_D = 5$ Hz $R_b = 400$ kb/s, and the block size of the RS code is 255.

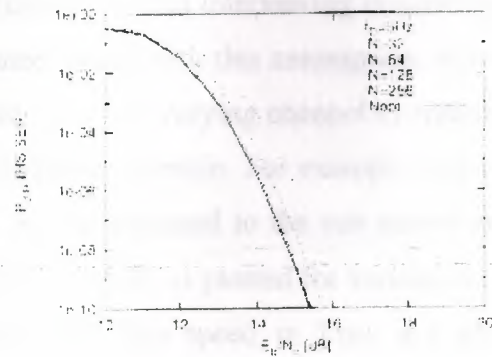


Fig.4.3. RS SER versus E_b/N_0 when $f_D = 5$ Hz, $R_b = 400$ kb/s, and the block size of the RS code is 255.

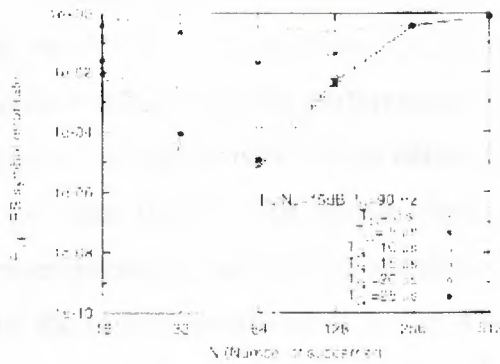


Fig.4.4. RS SER versus N when $f_D = 90$ Hz, $R_b = 400$ kb/s, and the block size of the RS code is 255.

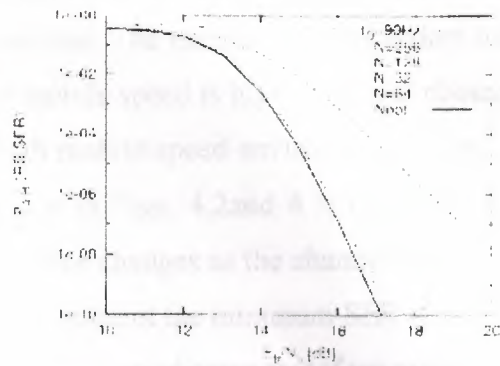


Fig. 4.5. RS SER versus E_b/N_0 when $f_D = 90$ Hz, $R_b = 400$ kb/s, and block size of the RS code is 255.

symbols. If we assume that 16-QAM symbols are perfectly interleaved, the RS SER before decoding is written as

$$P_{RS} = 1 - (1 - P_{16-QAM})^{1/2}$$

where P_{16-QAM} is the 16-QAM SER and

$$P_{16-QAM} \approx 10 P_{BPSK}$$

for Gray-mapped 16-QAM symbols. Although perfect interleaving is quite difficult to realize in practice, we can get the performance bound with this assumption. Moreover, the performance of interleaving can be improved in a slow varying channel by interleaving symbols not only in time domain but also in frequency domain. For example, one of two 16-QAM symbols which form one RS symbol can be allocated to the sub carrier and the other to the t th sub carrier. When (thus 400 kb/s) and 15dB, is plotted for various values of s and at the pedestrian (5 Hz) and high mobile (90 Hz) speed in Figs. 4.4 and 4.5, respectively. Since RS code rate varies as the value of s and varies, also varies in these figures. For example, when $s=1$, irrespective of the number of sub carriers when $s=1$, however, and for $s=2$ and $s=4$ respectively. We can see that there exist an optimum number of sub carriers that minimizes the post-decoding SER of the RS code for fixed total available bandwidth. This results from the tradeoff between the performance degradation due to increased ICI and the performance improvement due to increased error correction capability of RS code as the number of sub carriers increases.

Another observation from these figures is that, when the total available bandwidth is fixed, we should give first Priority to the guard interval. The number of sub carriers has a significant influence on the performance when the mobile speed is high: a careful choice of the number of sub carriers is thus demanded in high mobile-speed environments. Figs. 4.3 and 4.4 show the RS SER versus when As we saw in Figs. 4.2 and 4.3, there exists an optimum number of sub carriers and this optimum value changes as the channel states (and) vary: the solid lines labeled as in Figs. 4.4 and 4.5 represent the minimum SER obtainable when we use the optimum number. From Figs. 4.3 and 4.5 we observe that if we are allowed to switch from for the pedestrian speed to for high mobile speed (assuming the estimation of speed is possible), the performance can be improved considerably at the cost of some complexity compared to the case when we fix or irrespective of the speed.

CONCLUSION

Quadrature Amplitude Modulation (QAM) is a combination of amplitude modulation and phase shift keying. Modulation technique that varies both phase shift and amplitude Carrier frequency constant Data rates of 14,400, 19,200, 28, 800, 33,600 are possible Combining data compression and QAM can result in even higher throughput reaching, in some cases 128,000 bits per second. This scheme, used by most high speed modems, allows quicker data transfer than FSK. And it gives at least four states to send information. There's a good chance for our modem makes a dial up connection. IS-136 uses this technology to enable its digital control channel, allowing PCS like services for conventional cellular.

QAM allows us to obtain better separation between constellation points with a given amount of average signal power than a pure AM or PSK scheme for the same number of points M , and thus leads to better noise immunity.

The characteristics of the COFDM system can be varied to optimize the systems performance with different modulation schemes. While the most robust is QPSK, it has the limitation of only being able to achieve data rate of 10.6 Mbps

In Digital Television, 64-QAM is typical. 128-QAM and 256-QAM are also possible but require very accurate equipment to avoid bit errors when decoding takes place. As a greater number of amplitude and phase values are used, the system becomes progressively more prone to noise and attenuation during transmission.

REFERENCES

- [1] Feher, Applications of Digital Wireless Technologies to Global Wireless Communications, Prentice Hall 1997.
- [2] B. Widrow, J.R. Glover "Adaptive Noise Canceling: Principles and Applications," IEEE Proc., vol. 63, no.12, pp. 1692-1716, Dec. 1975
- [3] E.A Lee ,D.G. Messerschmitt "Static Scheduling of Synchronous Data Flow programs for Digital Signal Processing", IEEE Trans. on Computers, Vol. C-36, No. 1, Jan. 1987, pp 24-35.
- [4] H. Zou, H.J. Kim, S. Kim, B. Daneshrad, R. Wesel, W. Magione-Smith "Equalized GMSK, Equalized QPSK and OFDM, a Comparative Study for High-Speed Wireless Indoor Data Communications", IEEE Vehicular Tech. Conference 1999 (VTC'99)
- [5] Raymond Steele, Lajos Hanzo Mobile Radio Communication, Wiley 1999
- [6] D. Raychaudhuri, L. J. French, R. J. Syracuse, S. K. Biswas, R. Yuan P. Norseman, and C. A. Johnston" A prototype Raleigh fading of additive white Gaussian noise for wireless and wired QAM system for multimedia personal communication," IEEE J. Select. Areas Common, vol.15, pp. 83-95, Jan. 1997.
- [7] P. Key R , McFadden and M. Nilsson, "BER in QAM , positive and negative phase error Policing and Dimensioning" QAM Forum Contribution 97-0308, Chicago, 1997.
- [8] Fakhreddin Mamedov Telecommunication, Near East University, 2000